

Canadian Journal of Fisheries and Aquatic Sciences

Accounting for transient dynamics could improve the use of marine protected areas as a reference point for fisheries management

V.I. Quennessen @a, E.A. Babcockb, and J.W. White @a

^aDepartment of Fisheries, Wildlife, and Conservation Sciences, Coastal Oregon Marine Experiment Station, Oregon State University, 2030 SE Marine Science Drive, Newport, OR 97365, USA; ^bDepartment of Marine Biology and Ecology, Rosenstiel School of Marine, Atmospheric, and Earth Science, University of Miami, 4600 Rickenbacker Causeway, Miami, FL 33149, USA

Corresponding author: V. I. Quennessen (email: quennesv@oregonstate.edu)

Abstract

Biological reference points for fishery management depend on estimates of current stock status relative to unfished biomass (depletion). The ratio of fish density outside to inside a marine reserve, the density ratio, could serve as a proxy for depletion for data-poor management. However, transient dynamics associated with time lags in returning to the unfished state following reserve implementation make that proxy inaccurate on short time scales. We assessed density ratio management rules using an age-structured, spatially explicit model of four US west coast nearshore fishes following reserve implementation, with scenarios encompassing sampling error, recruitment variability, and uncertainty in natural mortality. In deterministic simulations, management incorporating time lags generally resulted in a higher mean and lower variability in biomass over 20 years, but lower mean yield compared to management that did not. However, when stochastic recruitment was included, differences among simulations due to stochasticity were much greater than any difference in performance between management strategies. Nonetheless, in certain cases, accounting for time lags could help avoid unwarranted increases in harvest effort after reserve implementation.

Key words: transient dynamics, density ratio, marine reserve, fisheries management, harvest control rule

Introduction

Fishery stock assessments use a variety of metrics, such as depletion relative to unfished spawning biomass or spawning potential ratio, to quantify the status of a stock relative to its unfished state. Stock status is then compared to management reference points, typically including a reference point for the desired target level of depletion and a limit below which harvest is curtailed to avoid threatening long-term population persistence (Restrepo 1999; Botsford et al. 2019). Harvest control rules, in turn, indicate the allowable fishing mortality, given the stock status in relation to the reference points. Generally, a higher fishing mortality is allowed if the stock is above a target reference point, and fishing mortality and catch are curtailed if the stock is below the target.

The successful use of any such assessment-based management strategy depends, in some way, on having an estimate of the unfished stock biomass or size structure, which requires long time series of catch and abundance data that are difficult to obtain for new or smaller, recreational fisheries (Wilson et al. 2010; Berkson and Thorson 2015), and for many datapoor nearshore species (Gunderson et al. 2008). This is further complicated by the fact that estimates of catch or biomass from the early history of fisheries are often not available (Dick and MacCall 2011) or were collected using different gear

or methodologies than present day. Moreover, conventional stock assessments are often developed at broad geographical scales larger than the scales at which population dynamics or fishing patterns could introduce heterogeneity in stock status (Botsford et al. 2009; McGilliard et al. 2011; Nickols et al. 2019; Berger et al. 2020). Finally, stock assessment results are often highly sensitive to the value of difficult-to-estimate natural mortality values and exploring that uncertainty is an important part of the precautionary approach (Punt 2006), though this is not always done (Garrison et al. 2011).

With about a third of the world's harvestable fish stocks being overexploited, depleted, or too data-poor to have an accurate status assessment (Beddington et al. 2007; Gutiérrez et al. 2011; Costello et al. 2012; FAO 2020), new fisheries management tools are needed that do not require long time series of data and are useful enough to inform adaptive precautionary management, even in the face of uncertainty (Gunderson et al. 2008; McGilliard et al. 2011). Marine protected areas (MPAs) can help inform fisheries management strategies by providing estimates for life history parameters such as natural mortality (Garrison et al. 2011), provide reference sites to aid in the management of marine resources, or be used as a buffer in the face of changing environmental conditions, such as those due to climate change (Wilson et al. 2020),

poorly implemented fishery management (De Leo and Micheli 2015), or natural disasters (Lubchenco et al. 2003). In one case, data from inside an MPA even provided for better management than the status quo quantitative stock assessment dependent on fishery data (Schroeter et al. 2001).

A harvest control rule that takes advantage of the growing number of fully no-take marine reserves, called the density ratio control rule, has been proposed by several authors (Wilson et al. 2010; Babcock and MacCall 2011; McGilliard et al. 2011). This density ratio acts as a proxy for stock depletion and is simply the ratio of population density outside to inside a marine reserve, or a fully no-take MPA (henceforth "reserve"). The portion of the stock outside represents the fished population, the portion inside represents an unfished population, and the density for each is calculated as the number of individual fish per unit area. Control rule-based management translates stock status to changes in fishing effort. Therefore, if an observed depletion level, or density ratio, is above some target density ratio that is set based on species life history and management goals, fishing mortality can safely increase; on the other hand, if the observed density ratio is below the targeted density ratio, fishing mortality would be reduced to allow the stock to rebuild. This metric is useful in that it does not require historical catch, abundance, or effort data, and can be applied at local spatial scales that are more appropriate for the management of smaller fisheries. Furthermore, it responds more readily to changes in stock productivity driven by environmental variability, instead of by fishing alone (Babcock and MacCall 2011). Despite these potential advantages, the density ratio approach has not been widely adopted.

One potential limitation of the density ratio harvest control rule is that it assumes the population within the reserve has fully recovered from fishing. Violation of this assumption can cause the control rule to inappropriately increase the allowable fishing effort if applied to a reserve where density is still influenced by historical fishing. It also does not take into account that instituting protections can lead to temporary fluctuations in population abundance, in part caused by time lags in the effect of the disruption of fishing pressure on the age structure of the population (Wilson et al. 2010; Babcock and MacCall 2011; McGilliard et al. 2011; Fenner 2012; White et al. 2013). Fishing pressure and increased total mortality, whether or not the fishery targets larger fish, often leads to the truncation of a population's age structure and the loss of old, large fishes (Barnett et al. 2017). With the reduction in fishing effort associated with reserve implementation, a gradual return to a size and age structure that includes a higher proportion of older fish is expected as the population in the reserve returns to its unfished state. However, this recovery can take decades, depending on life history and variability in reproduction (White et al. 2013; Kaplan et al. 2019). During that period, demographic lags in reproduction or recruitment failures preceding protection, or the loss of a reproductive portfolio effect that relies on older age classes (Anderson et al. 2008; Hsieh et al. 2010; White et al. 2013; Hopf et al. 2016; Arnold et al. 2018; Nickols et al. 2019), lead to dynamics, termed transient dynamics, that are different from stable, equilibrium dynamics. Potential transient dynamics

include an initial decrease in biomass or abundance immediately following protections. These transient dynamics complicate the short-term use of the density ratio as a reference point for the unfished state of the species. If these transient dynamics result in an initial decrease in abundance that is not considered, managing the fishery using conservative density ratio reference points may still lead to a collapse (McGilliard et al. 2011).

Results from age-structured modeling studies show that the eventual increase in abundance and biomass inside reserves depends on the level of fishing in that area prior to reserve implementation, and that the rate at which biomass increases and the age structure recovers increases with the species' natural mortality rate and decreases with the von Bertalanffy growth rate, variability in recruitment, and age at entry into the fishery (White et al. 2013; Kaplan et al. 2019). Most importantly, for populations of slow-growing fish, such as rockfishes (genus Sebastes) on the Pacific coast of North America, the transient period is expected to last 10–20 years, or more, and abundance may fluctuate greatly over that period (Kaplan et al. 2019). Different species will have varying timescales for this transition due to differences in life histories, so they should be managed separately, with respect to how the harvest control rule should be designed to respond to rebuilding. Therefore, accounting for both transient dynamics and life histories could prove integral to the feasibility of adaptive fisheries management using density ratios near newly implemented reserves.

In Babcock and MacCall's (2011) original analysis, yield (by year 20 at the latest) and biomass (by year 10) were drastically reduced as fishing mortality was allowed to increase too quickly too soon in the black rockfish scenarios for which effort was immediately allowed to increase. We predicted that incorporating a transient-instead of a static-target reference point would mitigate this initial loss of yield by more strongly restricting the increase of fishing mortality during the transient period and concurrently allow the biomass within the reserve to increase more quickly; this should lead to higher relative yields and biomass during the transient period compared to when managing with static reference points. Furthermore, different species should have different optimal control rules. For example, species with longer lifespans that mature later (i.e., "slower" life histories), should be managed more conservatively compared to species with shorter lifespans that mature faster (i.e., "faster" life histories), because we expected the age structure to fill back in at a rate that depends on the natural mortality rate (White et al. 2013). However, we also suspected that any mean differences in the relative performance of different control rules may be obscured by recruitment variability and sampling error, which may preclude accurate predictions of population dynamics following reserve implementation.

Here we used a management strategy evaluation approach (Punt 2006; Punt et al. 2016) to advance our understanding of how small-scale fisheries near marine reserves could be managed using harvest control rules based on the density ratio (Babcock and MacCall 2011; McGilliard et al. 2011). Our objective was to evaluate whether the density ratio approach is improved when transient population dynamics are

accounted for and determine how the success of alternative control rules depended on species' life histories. We used a spatially explicit, age-structured model to perform our analysis in a series of increasingly complex and realistic scenarios, starting with purely deterministic dynamics, then adding observation error and environmental stochasticity. We found that in purely deterministic simulations, management incorporating transient dynamics generally resulted in higher biomass, lower initial yield but higher cumulative yield for fish with faster life histories, and lower variability in both biomass and yield. However, when stochastic recruitment was included, differences among simulations due to stochasticity was much greater than any difference in performance between management strategies.

Methods

Model overview

Following the steps of a management strategy evaluation, we simulated the true dynamics of a metapopulation that spans a reserve and adjacent fished areas (the operating model), simulated sampling from both the reserve and fished parts of the metapopulation to calculate the observed density ratio as a measure of stock status (the sampling model), and used that estimate to determine the fishing effort to be applied to the true fished population (the management model). We then examined how different types of observation and management models affected the fishery control rules and thus the ultimate level of yield obtained. Our analysis was focused on (1) determining whether density ratio control rules that accounted for transient populations dynamics would outperform those that do not and (2) quantifying the sensitivity of the density ratio control rule approach to observation and process error. Observation error was modeled by including estimating error in the sampling model rather than using perfect information from the operating model, and process error was in the form of recruitment variability in the operating model. For each combination of species, target density ratio, and error scenario, we simulated the use of a static control rule, in which the target density ratio remained constant through time after reserve implementation (as in the original analyses of density ratio management; Babcock and MacCall 2011 and McGilliard et al. 2011), and a transient control rule, in which the target density ratio shifted over time, to take into account the transient dynamics resulting from the implementation of a marine reserve and the subsequent shift in fishing pressure. Note that the calculated density ratio is the same for both kinds of control rules, the only difference is the target density ratio to which it is compared, and whether it changes over time or not immediately following reserve implementation. In the case of potential uncertainty around the value of natural mortality, the management model also incorporated transient density ratio target values calculated using a potentially mis-specified value of natural mortality leading to a range of harvest control rules (Punt 2006). Estimates of natural mortality were set as 0.05 (in units of year⁻¹) above and below the "true" estimate; we set this value in light of estimated interquartile ranges for realistic

uncertainties in stock assessments for data-poor species, both with and without adult movement (Garrison et al. 2011). For our four nearshore study species, black rockfish (Sebastes melanops, Sebastidae), cabezon (Scorpaenichthys marmoratus, Cottidae), lingcod (Ophiodon elongatus, Hexagrammidae), and canary rockfish (Sebastes pinniger, Sebastidae), this represented a 29%, 19%, 18%, and 96% change in natural mortality, respectively.

In the simulated environment, there were five adjacent spatial patches along a theoretical linear coastline, where movement of adults occurred only between populations in adjacent patches, and the middle patch was designated to become a reserve, such that approximately 20% of the population was protected at any time. Thus, there is the potential for spillover from the reserve to the two adjacent patches, as well as spill-in as fish move from fished patches to the reserve. The boundaries of the entire model domain were nonperiodic and nonabsorbing, so no individuals were lost outside of the five patches. This was intended to represent a generic coastal metapopulation of arbitrary spatial extent, with habitat patches large enough to encompass adult movements but near enough to each other that larval connectivity was equal between all patches (Babcock and MacCall 2011). We assessed differences in biomass, yield, and effort immediately following reserve implementation for each species. To facilitate a comparison of our model outputs to previous work with the density ratio approach, many of the choices about the structure of the model mirrored those in Babcock and MacCall (2011). For a full description of the model functions and parameters, see Appendix A. The model was implemented in R version 3.5.3 (R Core Team 2019); code is available online (http://dx.doi.org/10.5281/zenodo.3970972).

Study species

We used four different nearshore species across a range of life histories-from slow life histories exemplified by low growth rates and high natural mortalities to faster life histories with high growth rates and low natural mortalitiesto explore the effects of incorporating transient dynamics on fisheries management immediately following reserve implementation. Each fishery is recreationally or commercially important on the US Pacific coast, and had different combinations of natural mortality and growth rate values, which influence the amplitude and longevity of transient dynamics (Ezard et al. 2010; Hastings 2016). The species modeled were black rockfish, canary rockfish, cabezon, and lingcod. We obtained life history and fishery selectivity parameters from the most recent stock assessments available for each (Cope et al. 2016, 2019; Thorson and Wetzel 2016; Haltuch et al. 2018). The models were age-structured, and length-age, length-biomass, and biomass-fecundity relationships were used to calculate biomass and fecundity (eqs. A1a-A3).

Model initialization

We set the initial conditions for the operating model at the stable, unfished age distribution. The population size of each age class was calculated as the number of individuals from the previous age class that survive, as well as the number of

individuals that survive in the current age class for the accumulator age bin (see eqs. A13 and A14). Fishing mortality had age-dependent selectivity (vulnerability to the fishery), which we based on the selectivity curves estimated in each stock assessment. We modeled selectivity as the weighted average of the selectivity curves for each commercial and recreational fleet described in the assessments (we did not include research and survey fleets), with weightings determined as the proportion of the fishery each fleet represented, calculated as the average proportion of catch over the three most recent years reported in the stock assessment. While individual fleets' selectivity curves were either dome-shaped or asymptotic, the overall selectivity at age for most species ended up dome-shaped, with some intermediate age being most vulnerable to the fishery, except for cabezon, where selectivity was greater than 0.875 for all ages after recruiting to the fishery (eqs. A8 and A9; Fig. A1). To initialize fishing effort, we evenly distributed a unitless amount of relative effort to each patch and began with an estimate of F that led to the depletion level reported in the most recent stock assessment. Here, depletion is defined as the ratio of spawning biomass to unfished spawning biomass (Cope et al. 2016).

After initialization at the stable unfished age distribution, we simulated 50 years of fishing with equal effort in each patch. Then, a reserve was established by setting the fishing effort in the middle patch to zero and redistributing the total effort equally among the remaining four patches. At the beginning of each simulated year, we reallocated fishing effort among patches according to the ideal free distribution principle (Fretwell and Lucas 1969), proportional to the previous year's yield, such that fishing effort was highest in the patch that had the highest yield in the previous year (eq. A10). Then, for each pair of adjacent patches, 10% of adult fish in each patch moved to the other, in both directions (eqs. A5-A7). Demographic parameters did not change between patches or over time. For each control rule, model year, and patch, we reallocated fishing effort, simulated movement of adults to adjacent patches, where they reproduced and 10% of larvae produced in each patch recruited to each adjacent patch, applied fishing mortality based on last model year's sampling data, conducted sampling, calculated the density ratio, and updated the next model year's relative effort based on the current management control rule.

Population dynamics operating model

The population dynamics operating model stepped the population forward in time in one-year increments, updating the numbers at age, abundance, biomass, and spawning stock biomass based on the level of fishing mortality specified by the management model. The age-specific fishing mortality was calculated as a function of the current fishing effort, gear catchability, and selectivity (eqs. A11 and A12). Recruitment occurred after harvest in each time step and was based on the spawning stock biomass. Recruitment followed a larval pool approach, where larvae pooled from all patches were distributed equally among patches before undergoing Beverton–Holt density dependence based on the spawning stock biomass present in that patch and dispersal, where

10% of larvae produced in each patch recruited to each adjacent patch (eqs. A5-A7). For model runs with recruitment variability, we simulated random variation in larval mortality or transport independently in each patch and for each year by multiplying the deterministic number of recruits based on the spawning stock biomass by a random number drawn from a lognormal distribution (eq. A4). This was justified due to a lack of evidence for autocorrelation in recruitment for West Coast rockfishes (Dorn 2002) and the most recent stock assessments for all species (Cope et al. 2016, 2019; Thorson and Wetzel 2016; Haltuch et al. 2018). Then, the number of fish in each age class was stepped forward in time annually, with continuous and simultaneous application of fishing and natural mortality, with a final accumulator age bin representing individuals of the maximum age and higher (eqs. A13-A15). We calculated abundance as the total number of individuals across all ages, and biomass as the weight (in kg) of the whole stock. Finally, we calculated the spawning stock biomass as the sum of the numbers at age multiplied by the maturity and weight at age. The catch (in units of numbers of individuals in each age class; eq. A16) and yield (total biomass of individuals caught, in kg) was calculated based on the agespecific fishing mortality rate in each patch according to the Baranov catch equation (Branch 2009; Botsford et al. 2019).

Sampling model

The sampling model simulated fishery-independent sampling of each patch. The sampling mimicked visual transect survey methods, such as those used to monitor reserves and fished sites on the US Pacific coast by the Partnership for the Interdisciplinary Studies of Coastal Oceans (PISCO) (Caselle et al. 2015; Menge et al. 2019). However, the sampling could also be imagined as hook-and-line scientific fishing surveys, or information from remote underwater video devices. Following the level of sampling that PISCO uses, there were 24 transects sampled in each patch in each model year. Simulated sampling in each year was a two-step process. First, there was a binomial probability of detecting any fish on each transect, which was calculated as a function of the proportion of positive transects observed during surveys, the estimated depletion level for the stock, and the proportional abundance in each patch (eqs. A17 and A18). Second, if there was a positive detection on a transect, then the count in each transect was estimated as a function of the mean count for positive transects in surveys, the estimated depletion for the stock, the total abundance in each patch, and a random normal variable used to model sampling error (eqs. A19 and A20). The parameters determining the probability of detection on survey transects (namely, proportion of positive transects) and the estimated counts on each positive transect (calculated using the mean and standard deviation of numbers of individuals identified on positive transects) were based on values used in the black rockfish assessment (Cope et al. 2016) and applied across all four species (Table A1).

After simulating the sampling process by estimating counts for each transect, we calculated the density ratio as the ratio of the average density of all fish outside to inside the reserve, where density was calculated as the sum of

estimated counts divided by the number of transects (eq. A21). There are other possible ways to calculate a density ratio (e.g., using only mature individuals, or only patches further away from the reserve); the method we used produced one of the best-performing control rules in Babcock and MacCall's (2011) analysis, so we did not explore other variations.

Management model and harvest control rules

After the creation of the reserve in year 0, the management model allocated the total fishing effort for subsequent years based on the calculated density ratio and which harvest control rule was in play. For each density ratio control rule, we allowed total fishing effort to increase linearly by 10% if the observed density ratio was above the target reference point, reduced effort linearly by 10% if the observed density ratio was below the target reference point, and we reduced effort to 10% of the initial effort if the observed density ratio fell below a floor value of 0.2 that was universal across all control rules. We chose a factor of 10% to facilitate comparison of our results with those of previous studies (Babcock and MacCall 2011). These control rules translated directly to changes in the next model year's total fishing effort, with the relative effort distributed in proportion to the previous years' yield.

For the transient control rules, the formula used to calculate the target density ratio at each time step was

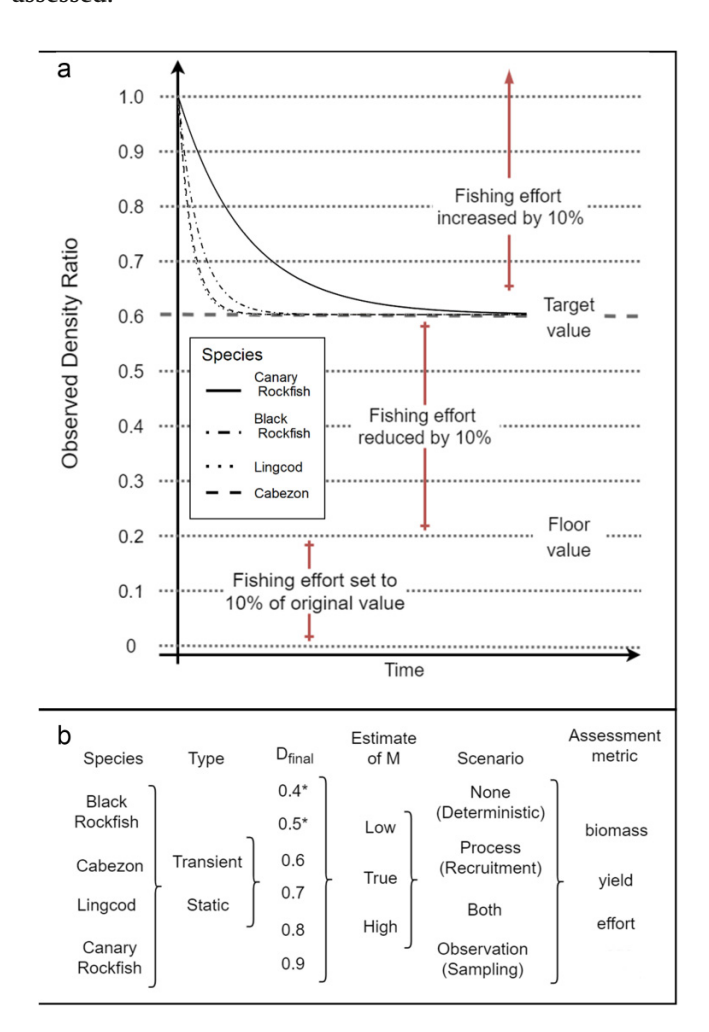
(1)
$$D(t) = 1 - (1 - D_{\text{final}}) (1 - e^{-Mt})$$

where D(t) was the target density ratio at year t, t was the time in years since reserve implementation, D_{final} was the final target density ratio, and M was the average natural mortality rate for a species (units year⁻¹). In this case, the target density ratio changed over time, starting at 1 (reflecting the expectation that at the time of implementation, there should be no difference between reserve and fished areas) and gradually decreasing to the $D_{\rm final}$ value (as the population in the reserve increased in density), at which point the control rule transitioned to a static control rule. The rate at which the target density ratio decreased depended on natural mortality M, which is the rate at which a population "fills in" the age structure truncated by fishing after fishing ceases, as it returns to the unfished state (White et al. 2013). For most species, the target density ratio decreased to the D_{final} value within 20 years or less, except for the species with the slowest life history, canary rockfish (Fig. 1a), given the most recent estimates of natural mortality and a D_{final} value of 0.6.

Model implementation

We repeated the same simulations for each of the four model species. The $D_{\rm final}$ values simulated for each species were 0.4, 0.5, 0.6, 0.7, 0.8, and 0.9 (Fig. 1b). Note that higher $D_{\rm final}$ values, closer to 1, indicate that the density outside the reserve was closer to the density within the reserve, signifying a lower, more conservative level of fishing pressure. The $D_{\rm final}$ values of 0.4 and 0.5 were only presented for cabezon, because for the other species those values produced identical results as the $D_{\rm final}$ value of 0.6 over a 20-year time frame in deterministic simulations, and so were not included in figures. Finally, we simulated dynamics for populations that

Fig. 1. Model methods. Panel ashows the density ratio harvest control rules used in the model simulations for all four species with a floor value of 0.2 and a target density ratio value of 0.6 (canary rockfish as an unbroken line, black rockfish as a dot-dashed line, lingcod as a dotted line, and cabezon as a dashed line). Note that for static control rules, the target value stays the same over time (the thicker, gray, dashed line at y = 0.6), and for transient control rules, the target value decreases exponentially from 1 to the D_{final} , or final target density ratio value over time (the solid line), at a rate that depends on natural mortality. Panel b shows the factorial design for modeled simulations. The base model was simulated for each combination of species (black rockfish, cabezon, lingcod, and canary rockfish), type of control rule (static and transient), D_{final} value (0.4 through 0.9), and scenario (deterministic, sampling error only, recruitment variability only, and both recruitment variability and sampling error). Note that D_{final} values marked with asterisks (*) indicate simulations that were only visualized for cabezon due to their faster life history; for all other species, control rules with these two D_{final} values behaved the same as control rules with a D_{final} of 0.6, and so they were not visualized. For each combination, the resulting biomass, yield, and effort were assessed.



were managed with an annual fishing mortality rate (F) at or above maximum sustainable yield (current management practices: black rockfish F = 0.05; cabezon F = 0.17; lingcod F = 0.08; and canary rockfish F = 0.02) and for populations that were heavily overfished (black rockfish F = 0.16; cabezon F = 0.24; lingcod F = 0.16; and canary rockfish F = 0.04).

We modeled error as two separate processes in the model: (1) process error as recruitment variability in the population dynamics operating model, as reported in the most recent stock assessments (Cope et al. 2016, 2019; Thorson and Wetzel 2016; Haltuch et al. 2018) and (2) observation error as sampling error in the sampling model using estimated transect counts to calculate the observed density ratio instead of true abundance. Deterministic simulations had no recruitment variability or sampling error, and the density ratio was calculated based on the true abundances without measurement error (i.e., the sampling model was not implemented, and density ratios were calculated directly from the true values in the operating model; eq. A22). There were, therefore, four different observation scenarios: (1) deterministic simulations with no error or variability, (2) simulations with only recruitment variability, (3) simulations with only sampling error, and (4) simulations with both recruitment variability and sampling error. For a full list of parameters and equations used to simulate stochasticity in recruitment and sampling, see Appendix A.

We kept the value of many other parameters constant to limit the scope of this paper to influences of life history, type of control rule, D_{final} value, and the two sources of error. Quantities that were not varied and remained constant across simulations were the number of patches (five) and thus the proportion of habitat in the reserve (one patch, 20% of total); the total unfished recruitment (100 000); the floor density ratio (0.2); and the fish movement rate, which quantified the proportion of larvae and adults that moved to an adjacent patch each time step (10%). This value for movement was set for all species because previous work has shown that adult movement generally lessens the effectiveness of marine reserves in increasing biomass within reserves (Moffitt et al. 2009; Grüss et al. 2011), so we chose not to explore the sensitivity of our results to this parameter. For other parameters kept constant between species, see the bolded values in Table A1.

For each combination of species, type of control rule, and D_{final} value, we completed one deterministic simulation and 5000 stochastic simulations. This replicate value was determined via exploratory analyses, wherein we determined that running additional simulations beyond 5000 did not alter the variation in results.

Analysis of model output

The three response variables we report are total biomass (summed over all five patches), yield, and total fishing effort (both summed over the four fished patches). For each of these, we calculated relative values by dividing values at each timestep by the values the year the reserve was established (the last year when all patches were affected by fishing), and we extracted medians and interquartile ranges across all 5000

simulations for stochastic scenarios. Values greater than 1, therefore, indicated an increase in yield, biomass, or effort and values less than 1 indicated a decrease.

For deterministic simulations, we also calculated the cumulative mean and standard deviation of biomass and yield over 10 and 20 years following reserve implementation, and extracted the control rules, in terms of the type (transient or static) and D_{final} values, that led to the highest mean and lowest standard deviation values. Finally, for stochastic scenarios, we calculated the proportion of simulations where transient control rules led to higher response variables compared to their static counterparts, averaged over all scenarios and all 20 years.

Results

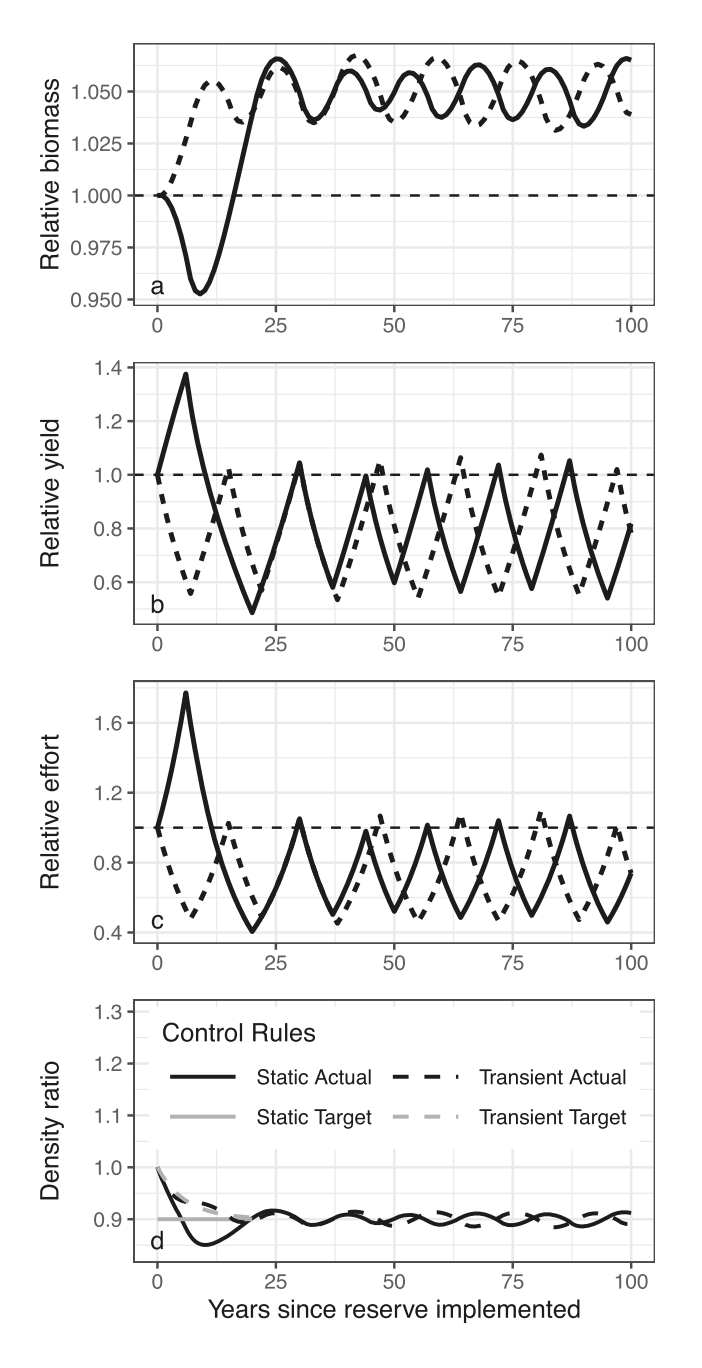
For space considerations, we focus on reporting results for black rockfish as a general example, because of their intermediate life history parameters (in terms of mortality and growth rates) and because differences between species were predictable based on life history. We present the additional results for canary rockfish, lingcod, and cabezon in the Supplementary Materials.

Deterministic simulations

A representative example of deterministic model results for a single D_{final} value of 0.9, simulated for 100 years after reserve implementation, shows that as the biomass and the abundance built up inside the reserve and fishing continued outside the reserve following implementation at t = 0, the density ratio decreased (Fig. 2). When the static control rule was in use, the observed density ratio started above the target, so the effort was allowed to increase—thereby allowing yield to increase and decreasing biomass-before effort was reduced after year 6. That, in turn, caused yield to decrease and allowed biomass to increase again. Because the transient target density ratio started at 1, the observed density ratio began just below the target after fishing began, so total effort was reduced in the first year following reserve implementation. This restricted yield and allowed biomass to increase without the same initial decrease seen when managed with a static control rule. In general, for the first 20 years, relative to the static control rule, the transient control rule led to lower relative effort and yield and a higher relative biomass. The long-term trend under both harvest control rules was an indefinite cycle in which the observed density ratio oscillates about the target value, producing equivalent but temporally lagged oscillations in effort, yield, and biomass. This cycle is due to the control rule always either increasing or decreasing effort in a given year.

The pattern depicted in Fig. 2 was generally shared across all species; relative biomass always increased initially for transient control rules and decreased initially for static control rules (Figs. 3a, S1-S3). Relative yield for static control rules was always greater than or equal to that for transient control rules immediately following reserve implementation (Figs. 3b, S1-S3). These differences in relative biomass and yield between static and transient control rules are because effort was always immediately restricted in the transient

Fig. 2. Curves show the deterministic biomass, yield, effort, and density ratio (vertical axis) over time (horizontal axis) for one hundred years following reserve implementation for black rockfish, given management using a $D_{\rm final}$ value of 0.9 for static (solid line) and transient (dashed) harvest control rules. Biomass, yield, and effort (summed over all patches and the fished patches, respectively) were scaled to be relative to their value in the year the reserve was implemented, such that a difference of 0.1 indicates a 10% change since that first year. The horizontal dashed line in panels a–c indicates no change in relative values after the reserve was implemented. The gray lines in panel d indicate the target density ratio over time (unbroken for the static control rule, dotted for the transient control rule).



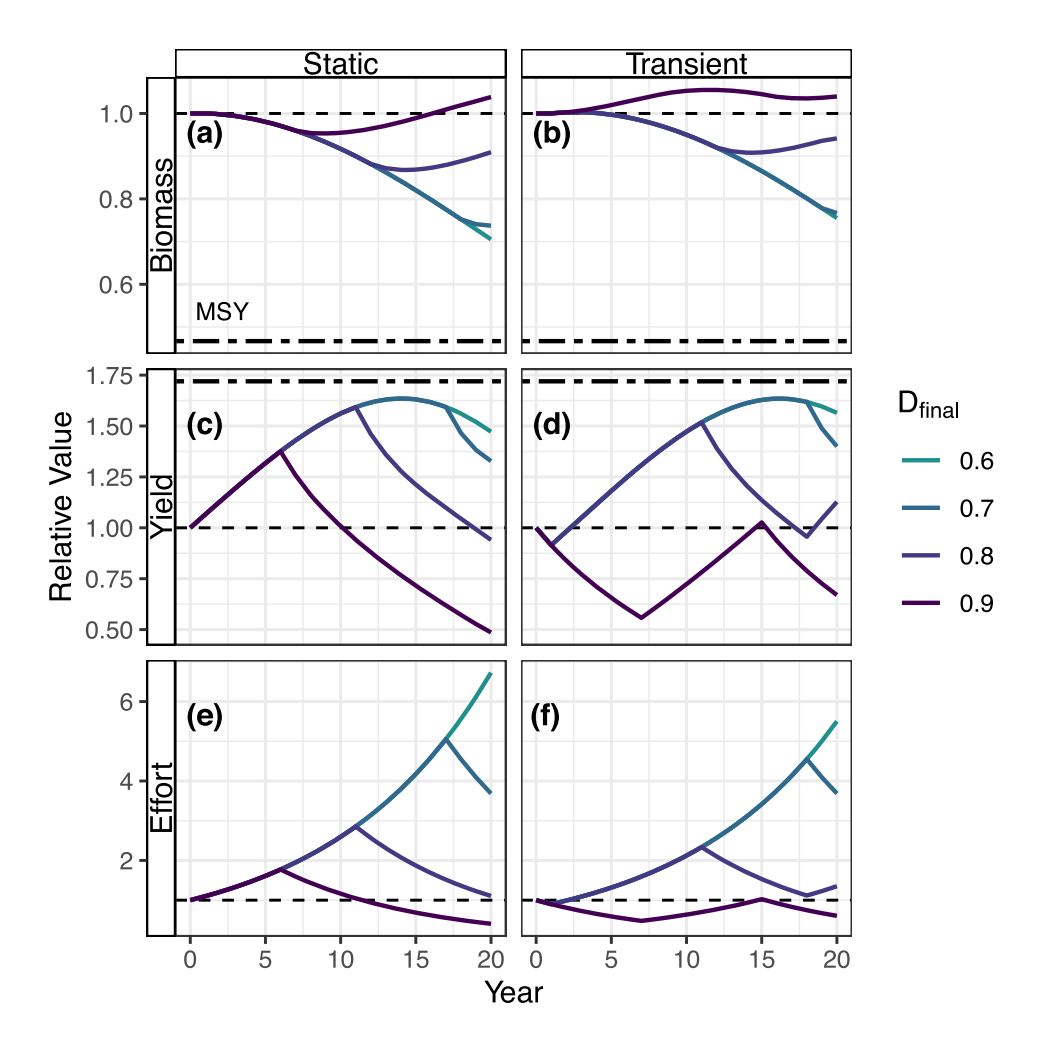
scenarios but initially allowed to increase in the static scenarios (Figs. 3c, S1–S3). Furthermore, within types of harvest control rule, control rules with higher D_{final} values had higher relative biomasses and lower relative yields for most of the timeframe (Figs. 3a, 3b, S1-S3). It is important to note that the most conservative control rules (i.e., with higher D_{final} values) always led to both the lowest and least variable effort. Extended simulations (100 years) showed that the general trend applied to canary rockfish over much longer timescales due to their slow life histories (Fig. S1). Across all species, transient control rules led to lower relative effort compared to static control rules, and as would be expected, more conservative control rules led to lower relative efforts compared to less conservative control rules in the first 20 years following reserve implementation. These patterns gave way to timelagged cycles in the first hundred years without any true difference in yield or biomass.

In general, transient control rules always led to an equivalent or higher biomass and an equivalent or lower yield over a 10- to 20-year period than static control rules with the same D_{final} values, except for cabezon with low D_{final} values $(D_{\text{final}} \leq 0.6; \text{ Fig. 4})$. However, these differences were greater for control rules with higher D_{final} values, and almost negligible for control rules with low D_{final} values. This is because cabezon is the only stock we considered that is currently estimated to be close to the biomass associated with maximum sustainable yield, so the control rule that allows effort to increase more actually decreases yield rather than increasing it. Conservative transient harvest control rules always led to the highest mean cumulative relative biomass by years 10 and 20 for all species except canary rockfish, for which all transient control rules performed equally well and led to a higher cumulative biomass than static control rules (Figs. 4a and 4b). However, the less conservative static control rules always led to the highest cumulative yield by years 10 and 20 for all species except for cabezon, where non-conservative transient control rules ($D_{\text{final}} = 0.5$ and 0.6) led to the highest cumulative yield in the short and long term, respectively (Figs. 4c and 4d). In general, transient control rules led to a higher standard deviation in biomass for canary rockfish and cabezon compared to the static control rules with the same D_{final} value (Fig. 5), but the transient control rule with a D_{final} value of 0.8 led to the lowest standard deviation for black rockfish and lingcod in both the short and long term (Figs. 5a and 5b). The patterns for yield were more complex, but the lowest cumulative standard deviation was generally a result of transient control rules of various D_{final} values except for lingcod in the short term (Fig. 5c). For the type and D_{final} value of the control rules that led to the highest cumulative mean and smallest cumulative standard deviation of biomasses and yields for all species and timeframes, see Table 1.

Effects of uncertainty in natural mortality estimates

Overall, the identities of the $D_{\rm final}$ control rule values that led to the highest cumulative biomass were not changed by bias in M. When the estimate of M used in the transient control rule was biased high (relative to the true value),

Fig. 3. Curves show the deterministic biomass, yield, and effort (vertical axis) for black rockfish over time (horizontal axis) for 20 years following reserve implementation for static control rules (left panels) and transient control rules (right panels). All response variables were scaled to be proportional to their value in the year the reserve was implemented, such that a difference of 0.1 indicates a 10% change since that first year. Curve color indicates the final target density ratio (D_{final}). The gray line at y = 1.0 indicates the biomass, yield, or effort at the time of reserve implementation, or year 0. The thick, two-dash line marks the relative biomass and yield that would result from constant fishing at F_{MSY} and is labeled "MSY" in panel a.



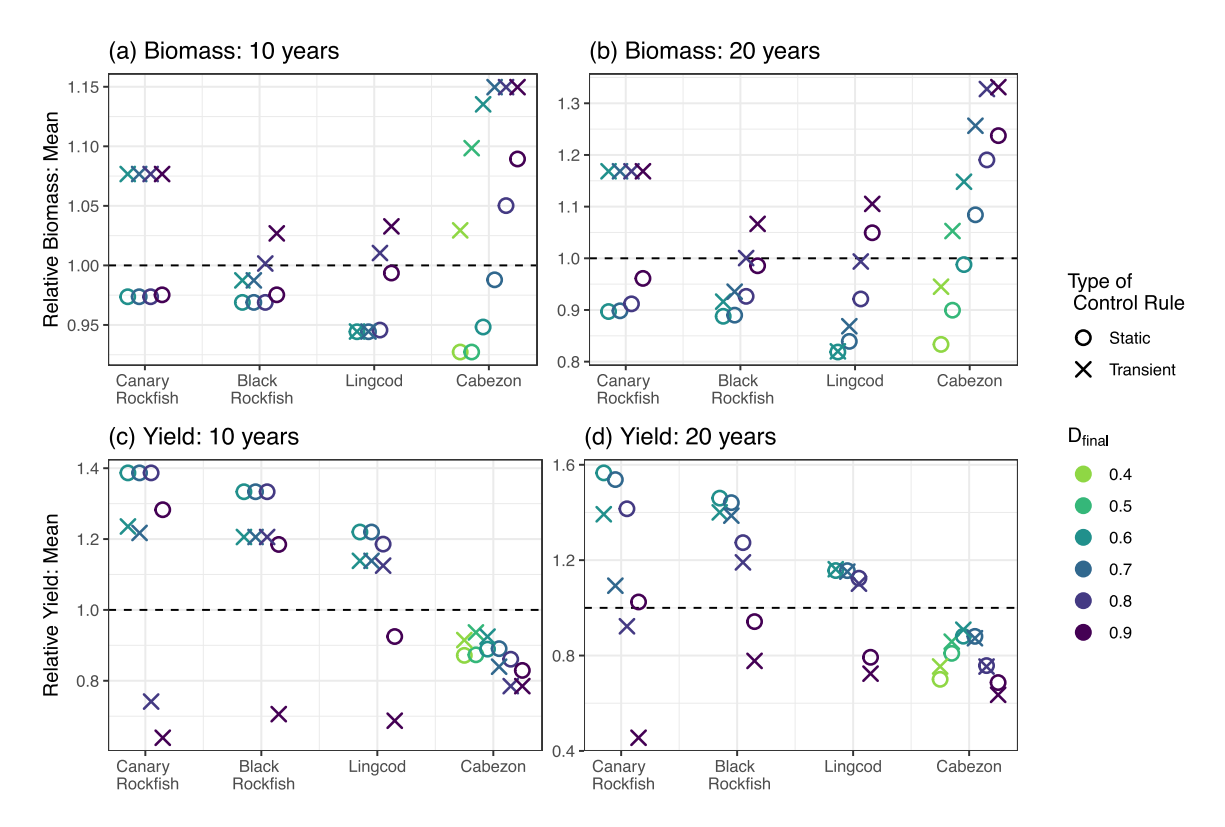
cumulative biomass remained constant or decreased relative to simulations with the correct value of M. Decreases were greater for lower D_{final} values, for both the short (10 years) and long term (20 years). Using a biased-low value of M led to slightly higher cumulative biomass relative to using the correct value (panels a and c in Figs. S4-S7). Furthermore, patterns in biomass and yield were the same as when M was known perfectly; for all control rules, estimates of natural mortality, and time frames, the static control rules led to lower cumulative biomass and higher cumulative yield compared to transient control rules with the same D_{final} values. Cumulative yield was constant or higher when M was biased high, relative to when the correct value was used (panels b and d in Figs. S4-S7). The exception was for less conservative control rules ($D_{\text{final}} \leq 0.5$) in cabezon, where cumulative yield was lower when estimated M was biased high (Figs. S7b–S7d). Further, static control rules generally led to the highest or almost highest cumulative yield, except for cabezon, where transient control rules with low to intermediate D_{final} values $(D_{\rm final} \leq 0.6)$ led to the highest cumulative yield (Figs. S7b–

S7d). While conservative D_{final} control rule values typically led to the highest yield in the long term when M was biased low, less conservative control rules led to the highest yield when M was biased high except for canary rockfish in the long term and for cabezon in the short term (Figs. S4-S7).

Simulations with only sampling error, only recruitment variability, and both sampling error and recruitment variability

Across stochastic scenarios (model runs incorporating the sampling model to estimate the density ratio, recruitment variability, and both sampling error and recruitment variability), transient control rules led to median decreases in effort and yield and increases in biomass for all species compared to static control rules with the same D_{final} value (Figs. 6, S8–S10). This mostly followed deterministic patterns, except that the transient control rule showed a higher yield by year 15 with deterministic simulations for black rockfish (Figs. 6d-6f) and started cycles of higher effort, yield, and

Fig. 4. Points show the cumulative mean relative biomass and yield over the short (10 years) and long term (20 years). Species are denoted along the horizontal axis and plotted points indicate (a) the mean cumulative biomass over the first 10 years, (b) the mean cumulative biomass over the first 20 years, (c) the mean cumulative yield over the first 10 years, and (d) the mean cumulative yield over the first 20 years for transient (marked with an X) and static (marked with an open circle) control rules, with different D_{final} values denoted by color. The dotted horizontal line demarcates a relative biomass or yield that is equivalent to the value the year the marine reserve was implemented, indicating no overall change.



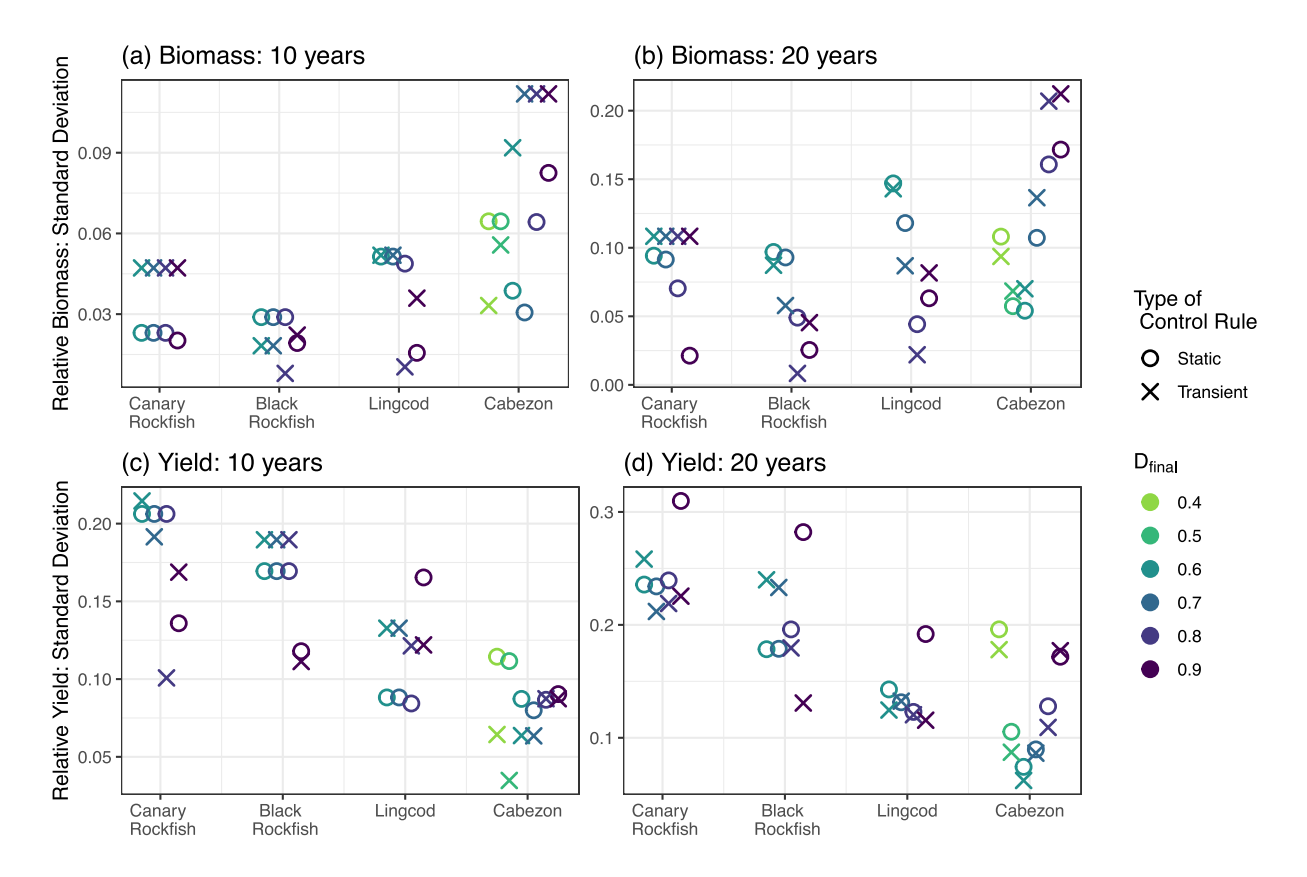
biomass produced by transient vs. static control rules sooner in lingcod and cabezon (Figs. S9 and S10). Furthermore, the interquartile ranges for each response variable overlapped considerably across harvest control rules for all four species (except for canary rockfish when only recruitment variability was incorporated, Figs. S8b, S8e, and S8h), indicating that whether a static or transient control rule could be expected to perform better in terms of in biomass or yield would depend in part on measurement uncertainty. Note that because we only plotted the control rules with the D_{final} value that led to the biggest difference between transient and static control rules at year 10 (D_{final} values of 0.8, 0.7, 0.8, and 0.5 for canary rockfish, black rockfish, lingcod, and cabezon, respectively), control rules with other D_{final} values have even more overlap.

The interquartile ranges for the transient and static control rules were overall larger with recruitment variability than when only adding sampling error. Furthermore, they overlapped across control rules for all metrics and all stochastic scenarios in all years for black rockfish, lingcod, and cabezon (Figs. 6, S9, and S10). For canary rockfish simulations with only recruitment variability, there was a strong separation in effort and yield years 6-18, which led to a delayed difference in biomass years 9-20 (Figs. S8b, S8e, and S8h). The interquartile ranges were of intermediate size between the scenarios with only sampling or only recruitment variability, indicating that by making it more difficult to correctly

estimate the density ratio in any given year, the sampling model did not consistently report high density ratios in early years and thus the management model did not ramp up effort in that time, dampening the eventual fluctuations in effort, yield, and biomass seen when only recruitment variability was modeled. In general, biomass in stochastic simulations was higher than that in deterministic simulations, and yield and effort were lower in the stochastic simulations than in deterministic simulations across all species and scenarios, with greater differences for scenarios with sampling error.

We similarly explored differences between transient and static harvest control rules with the lowest and highest D_{final} values for each species to evaluate whether differences due to the choice of target density ratio outweighed differences due to accounting for transient dynamics. Again, there was overlap in interquartile ranges of control rules with different D_{final} values for most metrics for most species across all stochastic scenarios (Figs. S11-S14). Across species, the overlap, in terms of both transient and static control rules with the same D_{final} value, as well as control rule with different D_{final} values, was greatest for simulations with sampling error and for black rockfish (Fig. S12) and lingcod (Fig. S13). For canary rockfish, there was a greater separation, potentially due to the stronger time lags caused by a lower natural mortality rate and overall slower life history (Fig. S11). For cabezon, the greater difference was potentially because of the

Fig. 5. Cumulative standard deviation of the relative biomass and yield over the short (10 years) and long term (20 years). Species are denoted along the horizontal axis and plotted points indicate (a) the cumulative standard deviation of biomass over the first 10 years, (b) the cumulative standard deviation of biomass over the first 20 years, (c) the cumulative standard deviation of yield over the first 10 years, and (d) the cumulative standard deviation of yield over the first 20 years for transient (marked with an X) and static (marked with an open circle) control rules, with different D_{final} values denoted by color. The dotted horizontal line demarcates a relative biomass or yield that is equivalent to the value the year the marine reserve was implemented, indicating no overall change.



greater difference between the most and least conservative control rule (Fig. S14). Across species, there was very little variation in relative effort for the least conservative static control rule, potentially because effort was allowed to increase across most simulations (Figs. S11–S14). Overall, the distributions of simulated biomass, yield, and effort overlapped greatly between static and transient harvest control rules across all species for the duration of simulations, such that any differences due to stochasticity were greater than any difference in performance between management strategies.

For simulations that were overfished, patterns in relative effort, yield, and biomass between static and transient control rules, and between control rules with different $D_{\rm final}$ values, were the same. However, populations that were originally overfished showed larger increases in biomass, larger decreases in yield that happened sooner, and lower increases in effort (Figs. S15 and S16).

Finally, we examined the proportion of simulations where managing with a transient control rule led to higher relative biomass, yield, and effort, as averaged across all stochastic scenarios and all 20 years. On average, transient control rules led to higher relative biomass (Fig. 7a), lower relative yield (except for cabezon with $D_{\rm final}$ values \leq 0.7; Fig. 7b),

and lower effort (Fig. 7c). Furthermore, except for cabezon, where the $D_{\rm final}$ value of 0.7 led to approximately 50% of simulations with higher yield when using transient control rules, as $D_{\rm final}$ values increased towards one, the proportion of runs approached 50%, indicating that there were smaller differences between response variable outcomes managed with static versus transient control rules (Fig. 7). Note that the results approximately mirror life history, such that a slower life history (lower M) leads to longer transients and a larger difference between static and transient control rules. However, there is also an effect of stock status at marine reserve implementation since the species managed closest to maximum sustainable yield (cabezon) showed an increase in yield for transient control rules relative to static control rules when the $D_{\rm final}$ value was low enough.

Discussion

Prior research has suggested that marine reserves can inform the management of data-moderate or data-poor fisheries by providing an example of an unfished population, to improve estimates of the level of depletion in fished areas comparable to quantitative stock assessments (Wilson et al. 2010; Babcock and MacCall 2011; Garrison et al. 2011;

Table 1. Best performing control rules.

	Species	Year 10: type $(D_{\rm final})$	Year 20: type (D_{final})	
Highest mean				
Biomass	Canary rockfish	Transient (0.6, 0.7, 0.8, 0.9)	Transient (0.6, 0.7, 0.8, 0.9)	
	Black rockfish	Transient (0.9)	Transient (0.9)	
	Lingcod	Transient (0.9)	Transient (0.9)	
	Cabezon	Transient (0.7, 0.8, 0.9)	Transient (0.9)	
Yield	Canary rockfish	Static (0.6, 0.7, 0.8)	Static (0.6)	
	Black rockfish	Static (0.6, 0.7, 0.8)	Static (0.6)	
	Lingcod	Static (0.6, 0.7)	Transient (0.6)	
	Cabezon	Transient (0.5)	Transient (0.6)	
Lowest standard dev	iation			
Biomass	Canary rockfish	Static (0.6, 0.7, 0.8)	Static (0.9)	
	Black rockfish	Transient (0.8)	Transient (0.8)	
	Lingcod	Transient (0.8)	Transient (0.8)	
	Cabezon	Static (0.7)	Transient (0.6)	
Yield	Canary rockfish	Transient (0.8)	Transient (0.7)	
	Black rockfish	Transient (0.9)	Transient (0.9)	
	Lingcod	Static (0.8)	Transient (0.9)	
	Cabezon	Transient (0.5)	Transient (0.6)	

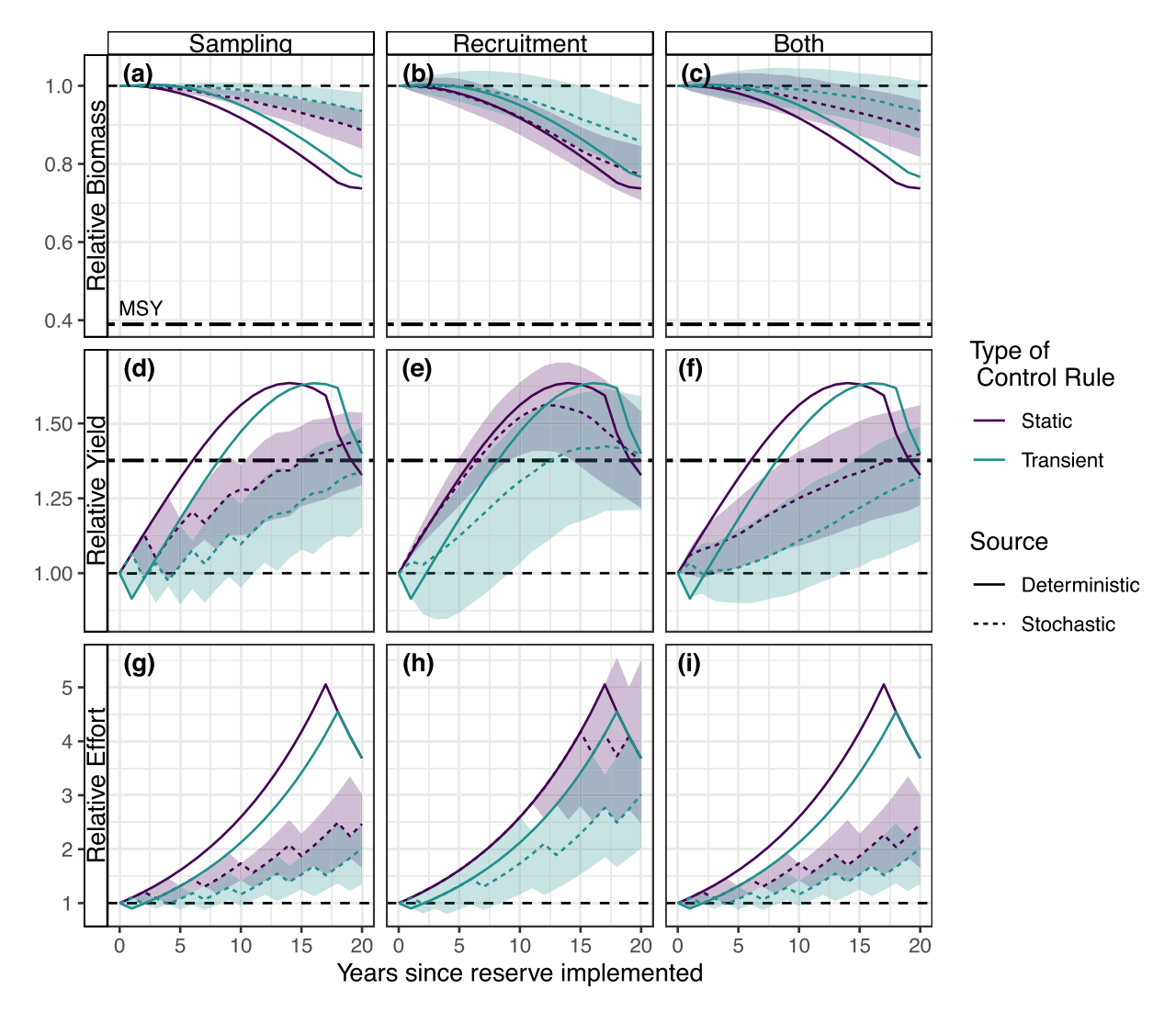
Note: Values denote the type (static or transient) and $D_{
m final}$ values of the control rule that resulted in the highest cumulative mean or lowest cumulative standard deviation for biomass and yield for each species over the first 10 and 20 years after reserve implementation. Control rules designated by more than one type or $D_{\rm final}$ value indicate that several control rules performed equally well.

McGilliard et al. 2011). However, one major criticism of previous modeling studies on this topic has been their focus on long-term outcomes (e.g., 50 years) rather than short-term consequences (first 10-20 years; Fenner 2012; McDonald et al. 2018). In essence, with any reserve implementation there will be shifts in fishing effort and exploitation rates, as well as an initial decrease in yield lost from the new reserve area. Accordingly, there will be debate about how best to manage those changes to minimize the impact on the fishery and preserve sustainable stocks (e.g., Hopf et al. 2016). For example, McGilliard et al. (2011) showed that density-ratio-based management using marine reserves as a reference point produced desirable outcomes in the long term but risked allowing overexploitation immediately after reserve implementation. To address this problem of short-term impacts, we examined harvest control rules that considered transient changes in stock size and structure in MPAs after implementation, as the population recovers its unfished age structure.

In deterministic simulations, a transient harvest control rule based on the ratio of abundance outside to inside a reserve that accounted for time lags in recovery had better outcomes in terms of total population biomass over both short and long time scales, relative to a static harvest control rule. Furthermore, transient control rules generally led to the lowest standard deviation in biomass for all species except cabezon and yield for all species by year 20. This was a promising outcome. However, the mean cumulative yield was lower and variability in yield was generally higher for the first 20 years for most species and management scenarios (with the exception of cabezon when managed with less conservative control rules). This would be undesirable for the economic stability of the fishery immediately following reserve implementation. Cabezon was often the exception because, of the four species studied, it is maintained closest to maximum sustainable yield (Cope et al. 2019). This aligns with the well-established theory that increased protections through MPAs show smaller increases, or indeed, sometimes decreases, in yield when the stocks are well managed to begin with (Holland and Brazee 1996; Jennings 2000; Benedetti-Cecchi et al. 2003; Hart 2006; Hilborn 2006; White et al. 2010; Edgar and Barrett 2012; De Leo and Micheli 2015).

Across all species, types of control rule, and error scenarios, transient and more restrictive density ratio control rules resulted in a higher total biomass and lower fishery yield in the first 10 years and higher relative yield at 20 years, on average. The underlying mechanism is that the abundances inside and outside the newly implemented marine reserves are very similar, leading to a high density ratio. Therefore, for static control rules, the effort is immediately allowed to increase, leading to an increase in yield and decrease in biomass until the harvest control rules are triggered. In the case of transient control rules, the time lags in the buildup of abundance are accounted for, and so the effort is not allowed to increase immediately, dampening the yield but allowing biomass to increase. Because it prevents the initial overshoot in effort and therefore yield, transient harvest control rules lead to long-term cyclic levels of yield and biomass faster than static control rules. Ergo, static control rules lead to a lower average biomass and higher average yield in the short term. However, in simulations that included both measurement error and recruitment variability, the distribution of possible outcomes under both static and transient harvest control rules overlapped considerably in most scenarios. Overall, accounting for transient dynamics led to earlier restrictions on fishing mortality rates and thus higher total biomass within 20 years of increased protections, as well as less extreme fluctuations

Fig. 6. Curves show the biomass (a-c), yield (d-f), and fishing effort (g-i) over time relative to the year the reserve was first implemented for black rockfish simulations, including recruitment variability, such that a difference of 0.1 indicates a 10% change since that first year. Results are shown for the D_{final} value that led to the greatest differences in biomass and yield between static and transient control rules by year 10 (color), and type of density ratio control rule (line type, static control rules are unbroken, transient control rules are dotted). Lines illustrate the median value across 5000 simulations, while the shaded region shows the interquartile range. Model simulations included observation error only (sampling error, panels a, d, and g), process error only (recruitment variability, panels b, e, and h), and both observation and process error (both recruitment variability and sampling error, panels c, f, and i). Note that for relative effort for static harvest control rules, the median value was also sometimes the minimum or maximum, hence the unusual appearance of the interquartile range. The gray line at y = 1.0 indicates the biomass, yield, or effort at the time of reserve implementation, or year 0. The thick, two-dash line marks the relative biomass and yield that would result from constant fishing at F_{MSY} and is labeled "MSY" in panel a.



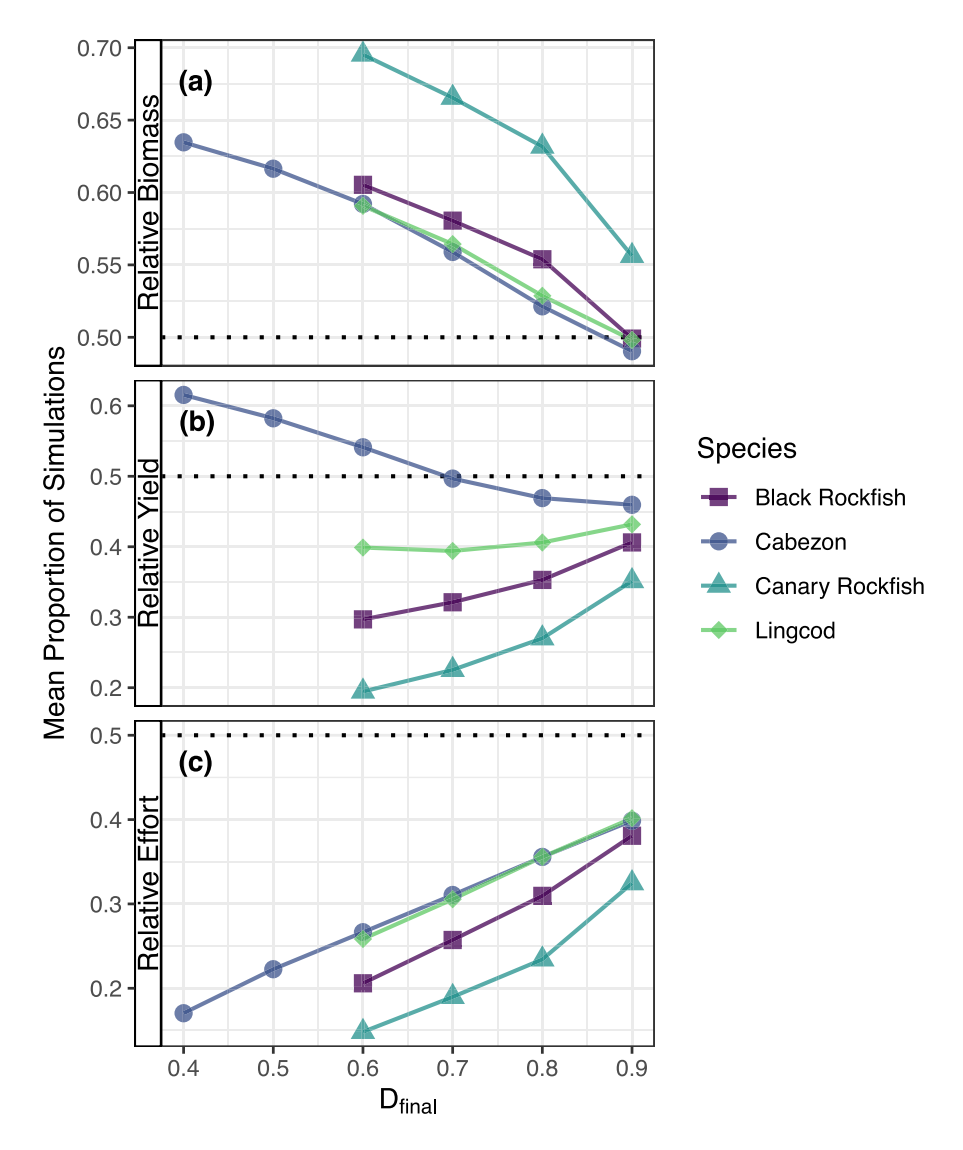
in fishing effort, but those restrictions generally produced lower cumulative and more variable yields for the first 10 and 20 years. Despite these general patterns, it was more often than not a transient control rule that led to the best yield, either in terms of highest mean or lowest variability, especially by year 20 (Table 1). Therefore, this method may be useful for managing for higher, stable yield in systems with lower interannual recruitment variability or very strong transient dynamics due to high historical fishing pressure or high natural mortality rates when using certain target density ratio values. Species with slower life histories (i.e., lower natural mortality and longer time to maturity) generally required a

higher final target density ratio to achieve the same management outcomes, due to longer time lags.

Previous management strategy evaluations used harvest control rules with a linear relationship between the observed density ratio and allowed fishing effort, with no lower threshold, and produced good long-term biomass and yields, but even the optimal control rule led to population decrease in the short term (i.e., 5-10 years following reserve implementation; McGilliard et al. 2011). This was because the harvest control rule allowed effort to increase too rapidly in that initial time period when the reserve was not yet representative of an unfished population (Wilson et al. 2010;

l of personal use of y.

Fig. 7. Lines show proportions of stochastic simulations where transient control rules led to higher values of response variables than static control rules, for different values of the final target density ratio, D_{final} . Results are shown for (a) relative biomass, (b) relative yield, and (c) relative effort. Values for different species were plotted in different colors and shapes (black rockfish as squares, cabezon as circles, canary rockfish as triangles, and lingcod as diamonds). The dotted line at y = 0.5 is the halfway point, above which transient control rules led to a greater proportion of higher than lower response variable outcomes. Results are pooled across all stochastic simulations; those with only recruitment variability, only sampling error, and both recruitment variability and sampling error.



McGilliard et al. 2011; Fenner 2012). In our model, accounting for the expected transient changes in the density ratio avoided that trap. We also found that harvest control rules with more conservative final target density ratios (i.e., a higher ratio of abundance outside to inside reserve) led to higher biomass and fishery yield over long time scales, relative to less conservative target density ratios, in agreement with previous analysis (Babcock and MacCall 2011). Additionally, more responsive changes in effort than a binary 10% increase or decrease could be explored in the future to reduce fluctuations in biomass and yield following reserve implementation. One major limitation of any control rule based on density ratios is the need for large, annual samples, which may be prohibitively expensive to collect (Dowling et al. 2019). Potential solutions for smaller sample sizes include

using a running average of the density ratio instead of annual estimates, or incorporating more sources of information, such as catch size distributions for exploited species.

The fact that including recruitment variability in simulations masks differences among management strategies in the trajectory of biomass and yield following reserve implementation agrees with hypotheses proposed by previous studies (De Leo and Micheli 2015). This is also supported by findings that differences in abundance, biomass, or yield between fished and protected areas, such as by a fully protected marine reserve, may not be detectable for more than 20 years in temperate systems such as the one we modeled (White et al. 2013; Starr et al. 2015; Kaplan et al. 2019; Nickols et al. 2019). The disparity between optimal control rules when managing for yield outcomes in the short term versus the

long term is supported by analyses that emphasizes the longterm gains for the fishery are often accompanied by shortterm losses after reserve implementation (Hastings and Botsford 2003; Hopf et al. 2016; Ovando et al. 2016). For example, Barceló et al. (2021) showed that the increase in yield in fished areas due to spillover of larvae produced in a reserve should have considerable time lags associated with first the buildup of reproductive biomass inside the reserve, and then the time for new recruit cohorts in fished areas to grow into the fished population (Barceló et al. 2021). Perhaps the only way to avoid that tradeoff is by removing fishing effort, such as with a buyout program (Hopf et al. 2016). This is effectively what is happening with the transient control rules for cabezon—because effort is reduced immediately, the population gets to its higher long-term yield faster than with the static control rule that overshoots effort before dialing back into the stable, cyclic yield and biomass values.

In examining the relative benefits of time-varying target density ratio targets, we made some simplifying assumptions about the dynamics of the fishing fleet itself. This was done to limit the dimensionality of the question at hand, but some aspects of this problem would be interesting topics for future analysis. In our model, fishing effort allocation assumed perfect information within the fleet about spatial yield distributions, and did not model separate economic drivers (e.g., fishery profit and costs of fishing effort) that could alter the actual distribution of effort in a given year (Sanchirico and Wilen 2001; White et al. 2008). It is possible that including some of those economic factors would have dampened some of the extreme fluctuations in yield and steady increases in fishing effort seen in our deterministic simulations. Those extreme increases in effort did not appear in the stochastic simulations because the density ratios fluctuated over time rather than exhibiting monotonic increases or decreases. This adds to our confidence in the stochastic simulations as more realistic representations of likely outcomes. Moreover, our analysis does not take habitat quality into account, and both survey results and impacts of control rules would certainly differ based on where the highquality habitat would be with respect to the marine reserve (Airamé et al. 2003; Friedlander et al. 2007; Ortiz and Tissot 2008; Claudet et al. 2010; Harford and Babcock 2016). Finally, it should be noted that these results are based on analysis of four nearshore groundfish stocks off the coast of Oregon, and so care should be taken in extrapolating beyond fisheries for moderately long-lived, sedentary species such as coral reef fish or other groundfish with its current implementation.

The density ratio control rule as we modeled it is an effortbased control rather than a catch-limit-based control, so it does not involve calculating allowable catch limits for stocks, as required for federal fishery management in the US. We took that approach because catch data are likely lacking for many coastal, recreational, and freshwater fisheries in the US, and for data-poor fisheries in general (e.g., Karr et al. 2015). Of course, if catch data were available, a densityratio control rule could be modified to incorporate it. With many countries expanding current MPAs and implementing new ones in accordance with Aichi Target 11 (Convention on Biological Diversity 2020), for any data-poor fisheries,

including many in the US, it may be beneficial to use a precautionary transient density ratio control rule to manage take of exploited populations. Babcock and McCall (2011) addressed the issue of developing multispecies density ratio control rules and found that they could produce overfishing of weaker species. For multispecies fisheries, we would expect that management would be dictated by the species with the poorest estimated stock status (Botsford et al. 2009) as is currently done for some multispecies groundfish fisheries in the US (Cope et al. 2011).

There are serious difficulties in managing data-poor fisheries, and density-ratio methods are one of several proposed solutions outlined in decision support systems such as Fish-Path (Dowling et al. 2016, 2019), among other methods that use empirical indicators such as taxonomy and life history parameters (Thorson et al. 2012), length metrics (Cope and Punt 2009), length frequency data (O'Farrell and Botsford 2005), or CPUE and size-based metrics (Wilson et al. 2010). The use of density ratio harvest control rules is best suited for systems where catch data are not readily available or consistent, but reserve monitoring data are available from both inside and outside the reserve. Our work suggests that modifying density-ratio-based harvest control rules to account for transient population dynamics leads to earlier reductions in fishery effort and lower effort overall, with modest reductions in short-term fishery yields and higher overall population biomass. This is in addition to performing as well as or better than other nondensity ratio harvest control rules, as compared in Babcock and MacCall (2011) and McGilliard et al. (2011). A potential benefit of this approach is the reduced risk of rapid increases in fishing effort after reserve implementation that could threaten population sustainability. Realistically, however, the success of any fishery management strategy depends on the degree of measurement error associated with assessments and its ability to accommodate process error in demographic rates such as recruitment. Overall, data-poor stock assessment frameworks, including those that apply density ratio harvest control rules, may be successfully applied as a viable scientific fishery management strategies for data-poor fisheries globally (Hilborn and Ovando 2014).

Acknowledgements

We thank S.A. Heppell, C. Wickham, and L. Ciannelli for guidance and comments on earlier versions of the manuscript, and R. Chen and two anonymous peer reviewers for constructive suggestions that improved the manuscript.

Article information

History dates

Received: 17 June 2022 Accepted: 14 September 2022

Accepted manuscript online: 20 September 2022 Version of record online: 29 November 2022

Copyright

© 2022 The Author(s). Permission for reuse (free in most cases) can be obtained from copyright.com.

Data availability statement

All model code can be found at http://dx.doi.org/10.5281/ zenodo.3970972

Author information

Author ORCIDs

V.I. Quennessen https://orcid.org/0000-0003-3626-5089 J.W. White https://orcid.org/0000-0003-3242-2454

Author contributions

VIQ: conceptualization, formal analysis, investigation, methodology, visualization, writing - original draft; EAB: methodology, writing - review & editing; JWW: conceptualization. funding acquisition, methodology, project administration, supervision, writing - review & editing.

Competing interests

The authors declare there are no competing interests.

Funding

This work was supported by the National Science Foundation (OCE-1909303), and VIQ was supported by the 2019 James Sedell Graduate Scholarship, the 2019 Oregon Lottery Graduate Scholarship, and the 2020 Chairman's Leadership Award funded by Ken Munson. This is contribution 525 from the Partnership for Interdisciplinary Study of Coastal Oceans funded primarily by the David and Lucile Packard Founda-

Supplementary material

Supplementary data are available with the article at https: //doi.org/10.1139/cjfas-2022-0125.

References

- Airamé, S., Dugan, J.E., Lafferty, K.D., Leslie, H., McArdle, D.A., and Warner, R.R. 2003. Applying ecological criteria to marine reserve design: a case study from the California Channel Islands. Ecol. Appl. 13(sp1): 170-184. doi:10.1890/1051-0761(2003)013[0170:AECTMR]2.0. CO;2
- Anderson, C.N.K., Hsieh, C., Sandin, S.A., Hewitt, R., Hollowed, A., Beddington, J., et al. 2008. Why fishing magnifies fluctuations in fish abundance. Nature, 452(7189): 835-839. doi: http://dx.doi.org. ezproxy.proxy.library.oregonstate.edu/10.1038/nature06851. PMID:
- Arnold, L.M., Smith, W.D., Spencer, P.D., Evans, A.N., Heppell, S.A., and Heppell, S.S. 2018. The role of maternal age and context-dependent maternal effects in the offspring provisioning of a long-lived marine teleost. R. Soc. Open Sci. 5(1): 170966. doi:10.1098/rsos.170966. PMID: 29410808.
- Babcock, E.A., and MacCall, A.D. 2011. How useful is the ratio of fish density outside versus inside no-take marine reserves as a metric for fishery management control rules? Can. J. Fish. Aquat. Sci. 68(2): 343-359. doi:10.1139/F10-146.
- Barceló, C., White, J., Botsford, L., and Hastings, A. 2021. Predicting the timescale of initial increase in fishery yield after implementation of marine protected areas. ICES J. Mar. Sci. 78(5): 1860-1871. doi:10.1093/icesjms/fsaa233. PMID: 33814897.
- Barnett, L.A.K., Branch, T.A., Ranasinghe, R.A., and Essington, T.E. 2017. Old-growth fishes become scarce under fishing. Curr. Biol. 27(18): 2843-2848.e2. doi:10.1016/j.cub.2017.07.069. PMID: 28918949.

- Beddington, J.R., Agnew, D.J., and Clark, C.W. 2007. Current problems in the management of marine fisheries. Science, 316(5832): 1713-1716. doi:10.1126/science.1137362. PMID: 17588923.
- Benedetti-Cecchi, L., Bertocci, I., Micheli, F., Maggi, E., Fosella, T., and Vaselli, S. 2003. Implications of spatial heterogeneity for management of marine protected areas (MPAs): examples from assemblages of rocky coasts in the northwest Mediterranean. Mar. Environ. Res. 55(5): 429-458. doi:10.1016/S0141-1136(02)00310-0. PMID: 12628195.
- Berger, A.M., Deroba, J.J., Bosley, K.M., Goethel, D.R., Langseth, B.J., Schueller, A.M., and Hanselman, D.H. 2020. Incoherent dimensionality in fisheries management: consequences of misaligned stock assessment and population boundaries. ICES J. Mar. Sci. 78(1): 155-171. doi:10.1093/icesjms/fsaa203.
- Berkson, J., and Thorson, J.T. 2015. The determination of data-poor catch limits in the united states: is there a better way? ICES J. Mar. Sci. 72(1): 237-242. doi:10.1093/icesjms/fsu085.
- Botsford, L.W., Brumbaugh, D.R., Grimes, C., Kellner, J.B., Largier, J., O'Farrell, M.R., et al. 2009. Connectivity, sustainability, and yield: bridging the gap between conventional fisheries management and marine protected areas. Rev. Fish Biol. Fish. 19(1): 69–95. doi:10.1007 s11160-008-9092-z.
- Botsford, L.W., White, J.W., and Hastings, A. 2019. Population dynamics for conservation. In Population Dynamics for Conservation. Oxford University Press. Available from: http://www.oxfordscholarship.co m/view/10.1093/oso/9780198758365.001.0001/oso-9780198758365 [accessed 7 April 2020].
- Branch, T.A. 2009. Differences in predicted catch composition between two widely used catch equation formulations. Can. J. Fish. Aquat. Sci. 66(1): 126-132. doi:10.1139/F08-196.
- Caselle, J.E., Rassweiler, A., Hamilton, S.L., and Warner, R.R. 2015. Recovery trajectories of kelp forest animals are rapid yet spatially variable across a network of temperate marine protected areas. Sci. Rep. 5(1): 1-14. Nature Publishing Group. doi:10.1038/srep14102.
- Claudet, J., Osenberg, C.W., Domenici, P., Badalamenti, F., Milazzo, M., Falcón, J.M., et al. 2010. Marine reserves: fish life history and ecological traits matter. Ecol. Appl. 20(3): 830-839. doi:10.1890/08-2131.1. PMID: 20437967.
- Convention on Biological Diversity. 2020, September 18. Aichi Biodiversity Targets. Secretariat of the Convention on Biological Diversity. Available from: https://www.cbd.int/sp/targets/ [accessed 3 March 2021].
- Cope, J.M., and Punt, A.E. 2009. Length-based reference points for datalimited situations: applications and restrictions. Marine and Coastal Fisheries 1(1): 169–186. doi:10.1577/C08-025.1.
- Cope, J.M., DeVore, J., Dick, E.J., Ames, K., Budrick, J., Erickson, D.L., et al. 2011. An approach to defining stock complexes for U.S. west $coast\ ground fishes\ using\ vulnerabilities\ and\ ecological\ distributions.$ N. Am. J. Fish. Manag. 31(4): 589-604. doi:10.1080/02755947.2011. 591264.
- Cope, J.M., Sampson, D., Stephens, A., Key, M., Mirick, P.P., Stachura, M., et al. 2016. Assessments of California, Oregon and Washington Stocks of Black Rockfish (Sebastes melanops) in 2015. National Marine Fisheries Service, Seattle, WA. Available from: https://www.pcouncil.org/documents/2016/03/assessments-of-califo rnia-oregon-and-washington-stocks-of-black-rockfish-sebastes-mel anops-in-2015-published-03-31-2016.pdf/.
- Cope, J.M., Berger, A.M., Whitman, A.D., Budrick, J.E., Bosley, K.M., Tsou, S., et al. 2019. Assessing Cabezon (Scorpaenichthys marmoratus) Stocks in Waters Off of California and Oregon, with Catch Limit Estimation for Washington State. Pacific Fishery Management Council, Portland, OR. Available from http://www.pcouncil.org/groundfish/stock-assess
- Costello, C., Ovando, D., Hilborn, R., Gaines, S.D., Deschenes, O., and Lester, S.E. 2012. Status and solutions for the world's unassessed fisheries. Science, 338(6106): 517-520. doi:10.1126/science.1223389. PMID: 23019613.
- De Leo, G.A., and Micheli, F. 2015. The good, the bad and the ugly of marine reserves for fishery yields. Phil. Trans. R. Soc. B 370(1681): 20140276. doi:10.1098/rstb.2014.0276.
- Dick, E.J., and MacCall, A.D. 2011. Depletion-Based stock reduction analysis: a catch-based method for determining sustainable yields for datapoor fish stocks. Fish. Res. 110(2): 331-341. doi:10.1016/j.fishres.2011. 05.007.

- Dorn, M.W. 2002. Advice on west coast rockfish harvest rates from Bayesian meta-analysis of stock-recruit relationships. N. Am. J. Fish. Manag. 22: 280-300. doi:10.1577/1548-8675(2002)022%3c0280: AOWCRH%3e2.0.CO:2.
- Dowling, N., Wilson, J., Rudd, M., Babcock, E., Caillaux, M., Cope, J., et al. 2016. FishPath: a decision support system for assessing and managing data- and capacity-limited fisheries. In Assessing and Managing Data-Limited Fish Stocks. Edited by T. Quinn, II, J. Armstrong, M. Baker, J. Heifetz and D. Witherell. Alaska Sea Grant, University of Alaska Fairbanks. doi:10.4027/amdlfs.2016.03.
- Dowling, N.A., Smith, A.D.M., Smith, D.C., Parma, A.M., Dichmont, C.M., Sainsbury, K., et al. 2019. Generic solutions for data-limited fishery assessments are not so simple. Fish Fish. 20(1): 174-188. doi:10.1111/
- Edgar, G.J., and Barrett, N.S. 2012. An assessment of population responses of common inshore fishes and invertebrates following declaration of five Australian marine protected areas. Environ. Conserv. 39(3): 271-281. doi:10.1017/S0376892912000185.
- Ezard, T.H.G., Bullock, J.M., Dalgleish, H.J., Millon, A., Pelletier, F., Ozgul, A., and Koons, D.N. 2010. Matrix models for a changeable world: the importance of transient dynamics in population management: transient dynamics and population management. J. Appl. Ecol. 47(3): 515-523. doi:10.1111/j.1365-2664.2010.01801.x.
- FAO. 2020. The State of World Fisheries and Aquaculture 2020. Food and Agriculture Organization of the United Nations. doi:10.4060/ ca9229en.
- Fenner, D. 2012. Challenges for managing fisheries on diverse coral reefs. Diversity, 4(1): 105–160. doi:10.3390/d4010105.
- Fretwell, S.D., and Lucas, H.L. 1969. On territorial behavior and other factors influencing habitat distribution in birds. Acta Biotheor. 19(1): 16-36. doi:10.1007/BF01601953.
- Friedlander, A., Brown, E., and Monaco, M. 2007. Defining reef fish habitat utilization patterns in hawaii: comparisons between marine protected areas and areas open to fishing. Mar. Ecol. Prog. Ser. 351: 221-233. doi:10.3354/meps07112.
- Garrison, T.M., Hamel, O.S., and Punt, A.E. 2011. Can data collected from marine protected areas improve estimates of life-history parameters? Can. J. Fish. Aquat. Sci. 68(10): 1761-1777. doi:10.1139/ f2011-073
- Grüss, A., Kaplan, D.M., Guénette, S., Roberts, C.M., and Botsford, L.W. 2011. Consequences of adult and juvenile movement for marine protected areas. Biol. Conserv. 144(2): 692-702. doi:10.1016/j.biocon. 2010.12.015.
- Gunderson, D.R., Parma, A.M., Hilborn, R., Cope, J.M., Fluharty, D.L., Miller, M.L., et al. 2008. The challenge of managing nearshore rocky reef resources. Fisheries, 33(4): 172-179. doi:10.1577/1548-8446-33.4. 172.
- Gutiérrez, N.L., Hilborn, R., and Defeo, O. 2011. Leadership, social capital and incentives promote successful fisheries. Nature, 470(7334): 386-389. doi:10.1038/nature09689. PMID: 21209616.
- Haltuch, M.A., Wallace, J., Akselrud, C.A., Nowlis, J., Barnett, L.A.K., Valero, J.L., et al. 2018. 2017 Lingcod Stock Assessment. Pacific Fishery Management Council, Portland, OR. Available from https://www.pcou ncil.org/stock-assessments-and-fishery-evaluation-safe-documents/.
- Harford, W.J., and Babcock, E.A. 2016. Aligning monitoring design with fishery decision-making: examples of management strategy evaluation for reef-associated fisheries. Aquat. Living Resour. 29(2): 205. doi:10.1051/alr/2016018.
- Hart, D.R. 2006. When do marine reserves increase fishery yield? Can. J. Fish. Aquat. Sci. **63**: 5. doi:10.1139/f06-071.
- Hastings, A. 2016. Timescales and the management of ecological systems. Proc. Natl. Acad. Sci. U.S.A. 113(51): 14568–14573. doi:10.1073/pnas. 1604974113. PMID: 27729535.
- Hastings, A., and Botsford, L.W. 2003. Comparing designs of marine reserves for fisheries and for biodiversity. Ecol. Appl. 13(sp1): 65-70. doi:10.1890/1051-0761(2003)013[0065:CDOMRF]2.0.CO;2.
- Hilborn, R. 2006. Faith-based fisheries. Fisheries, 31(11): 554-555
- Hilborn, R., and Ovando, D. 2014. Reflections on the success of traditional fisheries management. ICES J. Mar. Sci. 71(5): 1040-1046. doi:10.1093/ icesjms/fsu034.
- Holland, D.S., and Brazee, R.J. 1996. Marine reserves for fisheries management. Mar. Resour. Econ. 11(3): 157-171. doi:10.1086/mre.11.3. 42629158.

- Hopf, J.K., Jones, G.P., Williamson, D.H., and Connolly, S.R. 2016. Fishery consequences of marine reserves: short-term pain for longerterm gain. Ecol. Appl. 26(3): 818-829. doi:10.1890/15-0348. PMID: 27411253.
- Hsieh, C., Yamauchi, A., Nakazawa, T., and Wang, W.-F. 2010. Fishing effects on age and spatial structures undermine population stability of fishes. Aquat. Sci. 72(2): 165-178. doi:10.1007/s00027-009-0122-2.
- Jennings, S. 2000. Patterns and prediction of population recovery in marine reserves. Rev. Fish Biol. Fish. 10: 209-231. doi:10.1023/A: 1016619102955.
- Kaplan, K.A., Yamane, L., Botsford, L.W., Baskett, M.L., Hastings, A., Worden, S., and White, J.W. 2019. Setting expected timelines of fished population recovery for the adaptive management of a marine protected area network. Ecol. Appl. 29(6): e01949. doi:10.1002/eap.1949. PMID: 31188493.
- Karr, K.A., Fujita, R., Halpern, B.S., Kappel, C.V., Crowder, L., Selkoe, K.A., et al. 2015. Thresholds in Caribbean coral reefs: implications for ecosystem-based fishery management. J. Appl. Ecol. 52(2): 402-412. doi:10.1111/1365-2664.12388.
- Lubchenco, J., Palumbi, S.R., Gaines, S.D., and Andelman, S. 2003. Plugging a hole in the ocean: the emerging science of marine reserves. Ecol. Appl. 13(sp1): 3-7. doi:10.1890/1051-0761(2003) 013[0003:PAHITO]2.0.CO;2.
- McDonald, G., Campbell, S.J., Karr, K., Clemence, M., Granados-Dieseldorff, P., Jakub, R., et al. 2018. An adaptive assessment and management toolkit for data-limited fisheries. Ocean Coast. Manag. 152: 100-119. doi:10.1016/j.ocecoaman.2017.11.015.
- McGilliard, C.R., Hilborn, R., MacCall, A., Punt, A.E., and Field, J.C. 2011. Can information from marine protected areas be used to inform control-rule-based management of small-scale, data-poor stocks? ICES J. Mar. Sci. 68(1): 201-211. doi:10.1093/icesjms/fsq151.
- Menge, B., Milligan, K., Caselle, J., Barth, J., Blanchette, C., Carr, M., et al. 2019. PISCO: advances made through the formation of a large-scale, long-term consortium for integrated understanding of coastal ecosystem dynamics. Oceanography, 32(3): 16-25. doi:10.5670/oceanog. 2019.307.
- Moffitt, E.A., Botsford, L.W., Kaplan, D.M., and O'Farrell, M.R. 2009. Marine reserve networks for species that move within a home range. Ecol. Appl. 19(7): 1835-1847. doi:10.1890/08-1101.1. PMID: 19831073.
- Nickols, K.J., White, J.W., Malone, D., Carr, M.H., Starr, R.M., Baskett, M.L., et al. 2019. Setting ecological expectations for adaptive management of marine protected areas. J. Appl. Ecol. 56(10): 2376-2385. doi:10. 1111/1365-2664.13463.
- O'Farrell, M.R., and Botsford, L.W. 2005. Estimation of change in lifetime egg production from length frequency data. Can. J. Fish. Aquat. Sci. 62(7): 1626-1639. doi:10.1139/f05-064.
- Ortiz, D., and Tissot, B. 2008. Ontogenetic patterns of habitat use by reef-fish in a marine protected area network: a multi-scaled remote sensing and in situ approach. Mar. Ecol. Prog. Ser. 365: 217-232. doi:10.3354/meps07492.
- Ovando, D., Dougherty, D., and Wilson, J.R. 2016. Market and design solutions to the short-term economic impacts of marine reserves. Fish Fish. 17(4): 939-954. doi:10.1111/faf.12153.
- Punt, A.E. 2006. The fao precautionary approach after almost 10 years: have we progressed towards implementing simulation-tested feedback-control management systems for fisheries management? Nat. Resour. Model. 19(4): 441-464. doi:10.1111/j.1939-7445.2006. tb00189.x.
- Punt, A.E., Butterworth, D.S., Moor, C.L. de, Oliveira, J.A.A.D., and Haddon, M. 2016. Management strategy evaluation: best practices. Fish Fish. 17(2): 303-334. doi:10.1111/faf.12104.
- R Core Team. 2019. R: A Language and Environment for Statistical Computing. R Foundation for Statistical Computing, Vienna, Austria. Available from https://www.R-project.org/.
- Ralston, S., and O'Farrell, M.R. 2008. Spatial variation in fishing intensity and its effect on yield. Can. J. Fish. Aquat. Sci. 65(4): 588-599. doi:10. 1139/f07-174.
- Restrepo, V. 1999. Precautionary control rules in US fisheries management: specification and performance. ICES J. Mar. Sci. 56(6): 846-852. doi:10.1006/jmsc.1999.0546.
- Sanchirico, J.N., and Wilen, J.E. 2001. A bioeconomic model of marine reserve creation. J. Environ. Econ. Manag. 42(3): 257-276. doi:10.1006/ jeem.2000.1162.

- Schroeter, S.C., Reed, D.C., Kushner, D.J., Estes, J.A., and Ono, D.S. 2001. The use of marine reserves in evaluating the dive fishery for the warty sea cucumber (*Parastichopus parvimensis*) in California, U.S.A. Can. J. Fish. Aquat. Sci. 58: 10. doi:10.1139/f01-127.
- Starr, R.M., Wendt, D.E., Barnes, C.L., Marks, C.I., Malone, D., Waltz, G., et al. 2015. Variation in responses of fishes across multiple reserves within a network of marine protected areas in temperate waters. PLoS ONE, 10(3): e0118502. doi:10.1371/journal.pone.0118502. PMID: 25760856.
- Thorson, J.T., and Wetzel, C. 2016. The status of canary rockfish (Sebastes pinniger) in the California current in 2015. 682. National Marine Fisheries Service, Seattle, WA. Available from https://www.pcouncil.org/documents/2016/05/the-status-of-canary-rockfish-sebastes-pin niger-in-the-california-current-in-2015-march-2016.pdf/
- Thorson, J.T., Cope, J.M., Branch, T.A., and Jensen, O.P. 2012. Spawning biomass reference points for exploited marine fishes, incorporating taxonomic and body size information. Can. J. Fish. Aquat. Sci. **69**(9): 1556–1568. doi:10.1139/f2012-077.
- White, C., Kendall, B.E., Gaines, S., Siegel, D.A., and Costello, C. 2008. Marine reserve effects on fishery profit. Ecol. Lett. **11**(4): 370–379. doi:10.1111/j.1461-0248.2007.01151.x. PMID: 18205836.
- White, J.W., Botsford, L.W., Moffitt, E.A., and Fischer, D.T. 2010. Decision analysis for designing marine protected areas for multiple species with uncertain fishery status. Ecol. Appl. 20(6): 19. doi:10. 1890/09-0962.1.
- White, J.W., Botsford, L.W., Hastings, A., Baskett, M.L., Kaplan, D.M., and Barnett, L.A.K. 2013. Transient responses of fished populations to marine reserve establishment: transient dynamics in marine reserves. Conserv. Lett. 6(3): 180–191. doi:10.1111/j.1755-263X.2012.00295.x.
- Wilson, J.R., Prince, J.D., and Lenihan, H.S. 2010. A management strategy for sedentary nearshore species that uses marine protected areas as a reference. Mar. Coast. Fish. 2(1): 14–27. doi:10.1577/C08-026.1.
- Wilson, J.R., Bradley, D., Phipps, K., and Gleason, M.G. 2020. Beyond protection: fisheries co-benefits of no-take marine reserves. Mar. Policy, 122: 104224. doi:10.1016/j.marpol.2020.104224.

Appendix A

This appendix contains all of the life history parameters and model equations required to implement the model used for analyses. All model parameters were drawn from the most recent stock assessments for each model species (Table A1). For more specific definitions and the usage of these terms, see eqs. A1–A22 and their respective descriptions. The model is freely available for download from a public GitHub repository (http://dx.doi.org/10.5281/zenodo.3970972).

Natural mortality

The model was single sex, so natural mortality was taken as the average between female and male natural mortality when they differed. Mortality, M, was constant with age, so survival from age a to a+1 was e^{-M} .

Growth

Growth parameters were based on female values in stock assessments because they were used to calculate egg production. The von Bertalanffy growth model was used to determine length at age a, L_a , as a function of the asymptotic maximum length L_{∞} , and growth rate k, where L_{∞} was calculated as a function of two ages (A_1 and A_2), the corresponding lengths at those ages (L_1 and L_2), and the growth rate k:

(A1a)
$$L_{\infty} = L_1 + \frac{L_2 - L_1}{1 - e^{-k(A_2 - A_1)}}$$

(A1b)
$$L_a = L_{\infty} + (L_1 - L_{\infty}) e^{-k(a-A_1)}$$

Weight at age a, W_a , was a simple exponential relationship with length at age a, L_a :

$$(A2) W_a = a_w L_a^{b_w}$$

Maturity and reproduction

The proportion of mature individuals at age a, P_{mat}^a , was calculated as a logistic function of the slope of the maturity curve, K_{mat} , length at age a, L_a , and the length at which 50% of individuals were mature, L_{50} :

(A3)
$$P_{\text{mat}}^a = \frac{1}{1 + e^{K_{\text{mat}}(L_a - L_{50})}}$$

Age of 50% maturity was calculated as the first age over which the proportion mature at age was greater than or equal to 0.5.

Recruitment at time t in patch p, $R_{t,p}$ was calculated using a larval pool, such that recruits for each patch came from the spawning stock biomass across all patches, but density dependence occurred in each patch after settlement as a function of the SSB_p, spawning stock biomass in the patch, as seen in (Babcock and MacCall 2011, method IV in their Table 1; see Ralston and O'Farrell 2008 for the derivation of this model), and was a function of the total number of patches P, the unfished recruitment R_0 , the stock steepness h, the sum of the spawning stock biomass SSB across areas, the unfished biomass B_0 , and an error term at time t, ν_R^t , which was drawn from a normal distribution for each timestep t with mean zero and standard deviation σ_R :

$$(\text{A4}) \quad R_{t,p} = \left(\frac{1}{P}\right) \frac{0.8 R_0 h \sum_p \text{SSB}_p}{0.2 B_0 \left(1 - h\right) + \left(h - 0.2\right) \sum_p \text{SSB}} e^{\left(\nu_R^t - \frac{\sigma_R^2}{2}\right)}$$

Movement

The number of adults in each patch after movement occurred was calculated as follows, where $N_{t,p}$ is the population size at time t in patch p, D_A is the adult movement proportion, and R_t is the number of recruits at time t in patch p. This equation is mathematically identical to the number of larvae moving between patches in the same manner, with the larval displacement proportion D_L replacing D_A and the number of recruits R replacing the total population size N.

(A5)
$$N_{t,1} = (1 - D_A)N_{t,1} + D_AN_{t,2}$$

(A6)
$$N_{t,p} = (1 - 2D_A)N_{t,p} + D_A(N_{t,p-1} + N_{t,p+1})$$

(A7)
$$N_{t,P} = (1 - D_A) N_{t,P} + D_A N_{t,P-1}$$

Selectivity

The selectivity at age a, S_a was modeled as two logistic functions, the upcurve U_a and downcurve D_a , respectively,

Table A1. Life history parameters.

Value	Symbol	Black rockfish	Cabezon	Lingcod	Canary rockfish
Stock	_	Oregon	Oregon	Washington and Oregon	Oregon
Source	_	Cope et al. 2016	Cope et al. 2019	Haltuch et al. 2018	Thorson and Wetzel 2016
Age at recruitment to the fishery (year)	$a_{ m rec}$	3	4	3	3
Plus-group age (year)	a_{\max}	40	20	25	84
Natural mortality (year ⁻¹)	M	0.17	0.26^{*}	0.28*	0.052
Age 1 (year)	a_1	1	4	1	1
Length at age 1 (cm)	L_1	20.32	44.30	17.28	9.05
Age 2 (year)	a_2	40	20	20	20
Length at age 2 (cm)	L_2	49.67	63.35	120	60.05
von Bertalanffy growth parameter (year ⁻¹)	k	0.210	0.225	0.128	0.129
Weight at length coefficient (kg·cm ^{-bw})	a_w	2.6×10^{-5}	1.90×10^{-5}	2.76×10^{-6}	1.18×10^{-5}
Weight at length exponent	b_{w}	2.88	2.99	3.28	3.09
Length at 50% maturity (cm)	L_{50}	43.69	43.00	56.70	42.00
Slope of maturity curve	K_{mat}	-0.66	-0.70	-0.27	-0.25
Recruitment standard deviation (number of recruits)	$\sigma_{ m R}$	0.50	0.50	0.55	0.50
Steepness	h	0.77	0.70	0.70	0.77
Larval drift proportion	$D_{ m L}$	0.1	0.1	0.1	0.1
Adult movement proportion	D_{A}	0.1	0.1	0.1	0.1
Depletion	D	0.604	0.528	0.579	0.555
Associated fishing mortality (year ⁻¹)	F_{D}	0.05	0.17	0.08	0.02
Fleets	_	Trawl, live, dead, ocean, shore	Live, dead, ocean, shore	Trawl, fixed gear, WA rec., OR rec.	Trawl, non-trawl, rec., hake, research
Proportion of fishery	F_P	0.0001, 0.1679, 0.0982, 0.6979, 0.0358	0.6033, 0.0415, 0.3423, 0.0130	0.2872, 0.1379, 0.3253, 0.2496	0.3908, 0.3122, 0.2246 0.0295, 0.0429
Alpha (selectivity)	α	0.325, 0.4, 0.35, 0.65, 0.425	0.4, 0.33, 0.35, 0.9	0.25, 0.25, 0.55, 1	0.3, 0.6, 1, 1, 1
Upcurve halfway point (year)	$U_{ m H}$	7, 5, 5, 5, 3	3, 4, 2, 1	3, 5, 5, 3	5, 5, 4, 8, 1
Beta (selectivity)	β	0.25, 0.5, 0.4, 1.1, 0.5	0.35, 0, 0, 0.2	0.09, 0.3, 0.17, 0.15	1, 0, 1, 1, 0.08
Downcurve halfway point (year)	$D_{ m H}$	15, 13, 13, 12, 6.5	17, 1, 1, 3	15, 12, 10, 9	10, 50, 7, 11, 30
Final selectivity	$S_{\mathbf{f}}$	0.325, 0.05, -0.11, -0.25, 0.135	0.7, 1, 1, 0.07	0.07, 0, 0, 0	0.36, 1, 0.175, 0.65, 0.8
Proportion of positive transects	$T_{I\!\!P}$	0.77	0.77	0.77	0.77
Mean individuals seen in positive transects (numbers of fish)	T_X	15.42	15.42	15.42	15.42
Standard deviation of individuals seen in positive transects (numbers of fish)	T_S	16.97	16.97	16.97	16.97

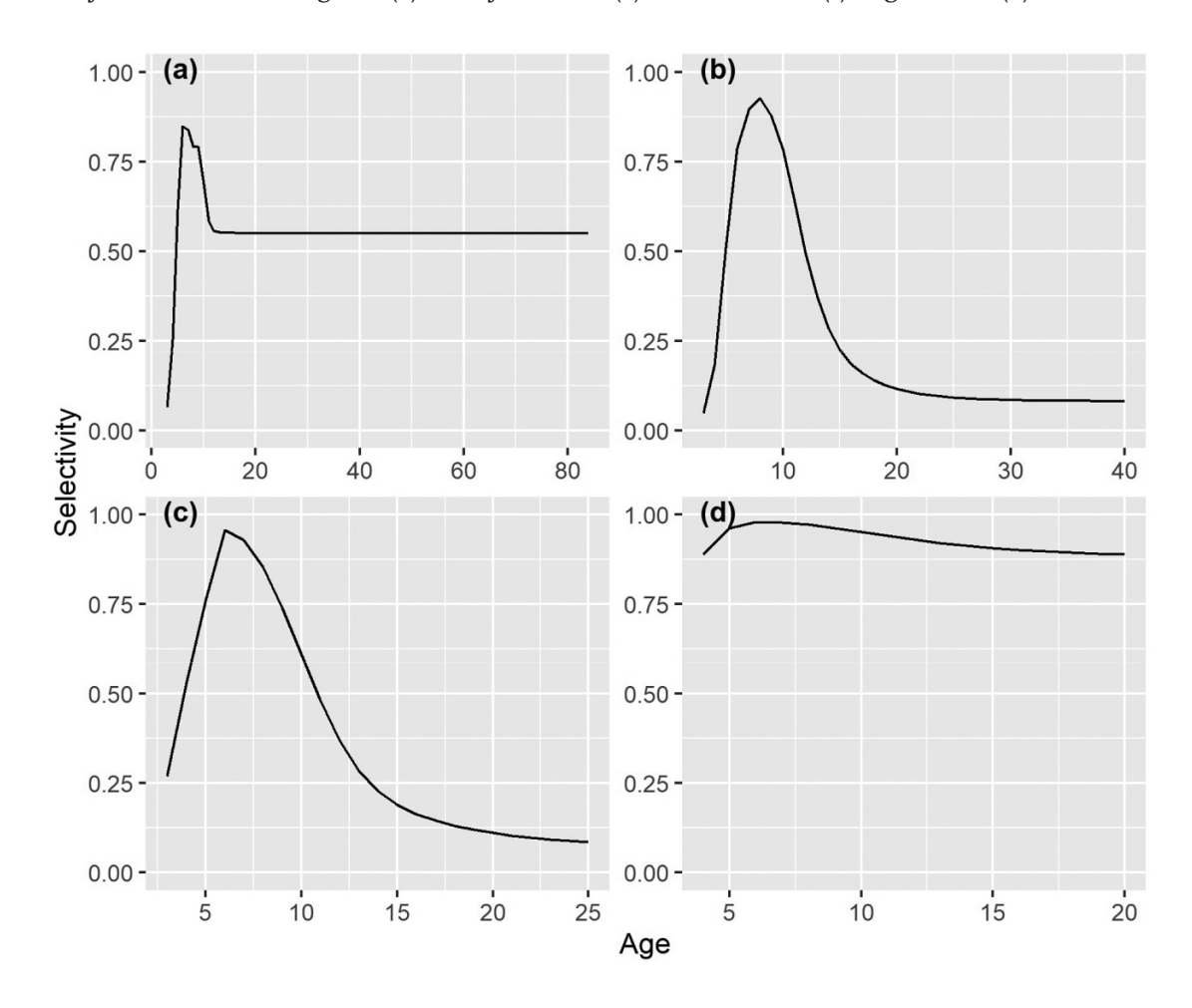
Note: Biological parameters used in the population dynamics model to evaluate transient effects on population dynamics and density ratio response in US west coast nearshore fisheries. Most parameters were obtained from the sources noted; boldface values indicate that the values were set to be the same across species, either due to lack of data for several species or to constrain factorial design of analysis. For Fleets, "rec." indicates a recreational fleet. Where stock assessments provided separate natural mortality values for males and females, an average value between the two sexes was used to simulate population dynamics and is demarcated by an asterisk (*). For complete definitions of all the terms, see eqs. A1–A22 and their accompanying descriptions.

which were modeled as a function of the logistic slopes α and β , the length at age a, L_a , and the length at the age at the midpoint of the upcurves and downcurves, $U_{\rm H}$ and $D_{\rm H}$, respectively. The maximum value between these two curves at each age determined the selectivity of that age class to

the fishery as a whole, based on the selectivity at length and length at age functions provided in the most recent stock assessments:

(A8)
$$U_a = \frac{1}{1 + e^{-1\alpha(L_a - U_H)}}$$

Fig. A1. Selectivity to all fisheries at age for (a) canary rockfish, (b) black rockfish, (c) lingcod, and (d) cabezon.



(A9)
$$D_a = \frac{1}{1 + e^{-1\beta(L_a - D_H)}}$$

Effort allocation

Effort was allocated according to the model of ideal free distribution, such that effort in each patch was proportional to the fraction of the yield caught in that patch in the previous year, as fishermen were more likely to fish where they had previously caught more fish. Reserve implementation was incorporated by setting the allowable effort in the reserve patch to zero, and redistributing the full effort to the other patches where fishing was allowed, again, according to the ideal free distribution (Fretwell and Lucas 1969), as a function of the yield in each patch, Yield $_{p,t}$, as well as total yield across patches and the currently estimated effort in each patch, Effort $_{v,t}$:

$$(A10) \quad \text{ Effort}_{t+1,p} = \frac{\text{Yield}_{t,p}}{\sum_{p} \text{Yield}_{t}} \text{Effort}_{p,t}$$

Stable age distribution

The stable age distribution was calculated as the numbers at age obtained after 150 years of population dynamics without any fishing pressure, i.e., with fishing effort set to zero. The first several years (equal to the age at recruitment), of the array for numbers at age were set equal to the stable age distribution.

Fishing mortality

The fishing mortality was calculated as a separate value for each age a and patch p, $F_{a,p}$, and was the product of three different values: the catchability at age a, V_a , the selectivity of individuals at age a to the fishery, S_a , and the unitless relative fishing effort for age a in patch p, $E_{a,p}$:

$$(A11) F_{a,p} = V_a S_a E_{a,p}$$

Where the vulnerability at age V_a was a function of the number of patches P, the historical fishing mortality for age a, F_h^a , and the sum of the fishing effort across all patches for age a, E_a :

(A12)
$$V_a = \frac{AF_h^a}{\sum E_a}$$

And where the historical fishing mortality was calculated based on a set of simulations where only population dynamics and fishing were applied to a population for 150 years, starting from the stable age distribution. Fishing mortality was set to values on the interval [0, 1], separated by 0.01. The historical fishing mortality that led to a depletion in year 150

that was closest to the depletion level reported in the most recent stock assessment was selected.

Population dynamics

Population size was initialized as the stable age distribution for the first several years. Due to the nature of the recreational fishery for each of the study species, where the fishing season was long and fish encounter fishing gear many times during the season, the continuous Baranov formulation was utilized to calculate catch (Branch 2009). For time steps greater than the age at recruitment, the numbers at age at recruitment were calculated using the recruitment function, and numbers at intermediate ages a and the final age bin n (respectively) were calculated based on the population size at the previous age at the previous timestep $N_{a-1,t-1}$ as well as the fishing mortality experienced by the previous age a-1 at the previous time step t-1, and natural mortality M:

(A13)
$$N_{a,t} = N_{a-1,t-1}e^{-1(F_{a-1,t-1}+M)}$$

(A14)
$$N_{a_{\max},t} = N_{a_{\max}-1,t-1} e^{-1(F_{a_{\max}-1,t-1}+M)} + N_{a_{\max},t-1} e^{-1(F_{a_{\max},t-1}+M)}$$

Note that because the annual natural mortality rate is not dependent on age, the population size N of any age class a, including those below the age at recruitment $a_{\rm rec}$, can be calculated as a function of the population size of age a at time t, the number of years n between age classes, and the natural mortality rate M:

(A15)
$$N_{a-n,t-n} = N_{a,t}/e^{M^n}$$

Catch and yield

Following eqs. A13 and A14, catch C was therefore a function of fishing mortality F, natural mortality M, and population size N, where C, F, and N were calculated for each age a, timestep t, and patch p:

(A16)
$$C_{a,t,p} = \frac{F_{a,t,p}}{F_{a,t,p} + M} N_{a,t,p} e^{-1(F_{a,t,p} + M)}$$

Sampling

The sampling function was modeled after the Partnership for the Interdisciplinary Studies of Coastal Ocean visual transect survey protocols, such that there were multiples of twelve transects per patch per year, distributed among two zones, three sides, and two depths (Caselle et al. 2015). Overall, 24 transects were modeled per patch per timestep. Transects were determined to be either positive or negative by pulling from a binomial distribution with a probability (Pr) which was the odds ratio for each patch (Odds $_p$), calculated as a function of the proportion of transects with a positive ID T_p , the stock depletion D, and the total abundance of fish in

patch p compared to the total abundance across all patches:

(A17) Odds
$$_p = \frac{T_P \text{ Abundance}_p}{D_p^1 \sum_p \text{ Abundance}}$$

$$(A18) \quad \text{ Pr} = \frac{1}{1 + e^{Odds}}$$

Once a transect had been either marked as positive or negative, an estimated species count for each positive transect in each patch p, the vector $Count_p$, was calculated as a function of the mean number of individuals identified on transects with a positive ID T_x , the stock depletion D, the abundance in patch p, and an error term calculated for each timestep t, v_s^t :

(A19) Count_p =
$$(T_X/D)$$
 Abundance_p $e^{v_S^t}$

Where the sampling error term v_S was drawn from a normal distribution with mean zero and standard deviation σ_s , calculated as a function of the mean and standard deviation of numbers of individuals observed on transects with positive IDs, T_x and T_s , respectively:

(A20)
$$\sigma_s = \sqrt{\ln\left[1 + \left(T_S/T_X\right)^2\right]}$$

Density ratio

The observed density ratio DR_{observed}, was calculated based on the total number of patches *P*, the sum of the counts outside and inside the reserve, Count_{outside} and Count_{inside}, respectively, and the total number of transects outside and inside the reserve, T_{outside} and T_{inside}, respectively:

(A21)
$$DR_{observed} = \frac{\frac{1}{(P-1)} \sum Count_{outside} / T_{outside}}{\sum Count_{inside} / T_{inside}}$$

The true density ratio DR_{true} was calculated based on the total number of patches P, and the total actual abundance of the population outside and inside the reserves, as determined by the operating model:

(A22)
$$DR_{true} = \frac{\frac{1}{(P-1)} \sum Abundance_{outside}}{\sum Abundance_{inside}}$$

Management

For transient control rules, the target density ratio in year t was calculated as a function of the final target density ratio $D_{\rm final}$, natural mortality M, and time (in years) since reserve implementation t (eq. 1).

At each time step, for each control rule, and for each final target density ratio, if the observed density ratio was greater than the target density ratio, the effort was allowed to increase by 10% for the next timestep. On the other hand, if the observed density ratio was less than or equal to the target density ratio, but above the floor value of 0.2, the effort was decreased by 10% for the next timestep. Finally, if the observed density ratio was less than or equal to the floor of 0.2, the effort at the next timestep was set to 10% of the effort at the year the reserve was implemented.